Final Technical Report
Covering Period from June 28, 2006 to March 27, 2007

DOE SBIR Phase I Research
Improving the Performance of Lithium Ion Batteries at Low Temperature
Grant No: DE-FG02-06ER84531
Topic: 19-A

Principal Investigator: Trung H. Nguyen
Staff Scientist: Peter Marren
EIC Laboratories, Inc.
111 Downey Street
Norwood, MA 02062

Collaborator: Dr. Kevin Gering
Idaho National Laboratory
2525 North Fremont Avenue
Idaho Falls, Idaho 84315

Prepared for

U.S. Department of Energy
DOE Project Officer: James Barnes
1000 Independence Avenue, S.W.
Washington, DC 20585-1290

April 20, 2007

Phase I Summary

The ability for Li-ion batteries to operate at low temperature (between -10^oC and -20^oC) is extremely critical for the development of energy storage for electric and hybrid electric vehicle technologies. Currently, Li-ion cells have limited success in operating at temperature below -10^oC. Electrolyte conductivity at low temperature is not the main cause of the poor performance of Li-ion cells ([1]). The formation of a tight interfacial film between the electrolyte and the electrodes has often been an issue that resulted in a progressive capacity fading and limited discharge rate capability. Excessive polarization concentration on the anode due to the SEI film could also lead to deposition of metallic Li during charging. Thus, it is critical to resolve the fading power and Li plating on charge at low temperature before Li-ion battery can be ready for the commercial market.

The objective of our Phase I work is to develop novel electrolytes that can form low interfacial resistance SEI films on carbon anodes and metal oxide cathodes. The nature of the SEI film is critical to the low temperature performance of the Li-ion cell. The surface SEI film should act as a protecting barrier between the electrolyte and anode. Yet, at the same time, the SEI film should allow facile transport of Li ions through the film to facilitate intercalation and de-intercalation of Li ions into and out of carbon.

Our main effort was to identify, evaluate and modify cell components such as electrolyte and electrode materials that can enhance low temperature performance of Li-ion cells but without compromising their room temperature performance and cycle life. Our goal is to develop and design novel electrolytes and advanced electrode components that will significantly improve the low temperature performance of Li-ion cell at temperatures below -10^oC.

From the results of our Phase I work, we are very excited to find that the interfacial impedance of Fluoro Ethylene Carbonate (FEC) electrolyte at the low temperature of -20^oC is astonishingly low, compared to the baseline 1.2M LiPF$_6$ EMC:EC:PC:DMC (10:20:10:60) electrolyte. We found that electrolytes formulations with fluorinated-carbonate co-solvent have excellent film forming properties and better de-solvation characteristics to decrease the interfacial SEI film resistance and facilitate the Li-ion diffusion across the SEI film. For example, the interfacial resistances for Li/MCMB half cell in 1.2M LiPF$_6$ FEC:EC:GBL:EP (10:15:25:50) are respectively 0.9Ω at both 20°C and -20^oC. For the baseline electrolyte EC:EMC:PC:DMC, the interfacial resistances are respectively 23 Ω and 950 Ω at 20°C and -20^oC. While the interfacial resistance of MCMB in the baseline electrolyte has increased by 40 times going from 20°C to -20^oC, the interfacial impedance in FEC electrolyte remained practically the same at -20^oC.

The very overwhelming low interfacial impedance for FEC electrolyte will translate into Li-ion cell with much higher power for cold cranking and high Regen charge at the low temperature. Further, since the SEI film resistance is low, Li interaction kinetics into the electrode will remain very fast and thus Li plating during Regen/charge period will less likely to happen.

Phase I Results

1- *Evaluation of new electrolyte formulations*

The purpose of this task is to screen potential electrolytes with fluorinated carbonates as co-solvents and the combination of $LiPF_6$/$LIBF_4$ as electrolyte salts. Electrolyte components were investigated to increase the interfacial reaction across the SEI film and to improve the charge/discharge rate of the Li-ion batteries at low temperatures.

Initially, we want to know to what extent the presence of mono-fluoroethylene carbonate (FEC) will affect the conductivity of the electrolyte mixture. Fluorinated solvents have significantly improved properties over their analogous non-fluorinated solvents, such as lower viscosity, lower melting point, and high stability toward oxidation. We have evaluated the electrolyte conductivities of the FEC co-solvent along with PC/DMC and EC.

We have used a statistical experimental mixture design to study the effect of FEC on electrolyte conductivities. To determine the sensitivity of our measurements with different conductivity cells, we have used three different cells with different cell constants for measuring the conductivity of the baseline electrolyte 1.2M $LiPF_6$ in EMC:EC:PC:DMC (10:20:10:60). Conductivity measurements were performed within the temperature range of +20 to -40°C. The results are reported in Table 1.

Table 1. Baseline conductivity measurements for establishing reproducibility

Electrolyte 1.2M $LiPF_6$ in EC:DMC:PC:EMC (10:20:10:60)

	20°C	0°C	-10°C	-20°C	-30°C	-40°C
Cell 3	1.23E-02	7.9E-03	6.2E-03	3.7E-03	8.6E-04	7.1E-05
Cell 4	1.15E-02	7.0E-03	6.1E-03	3.1E-03	8E-04	6.6E-05
Cell 6	1.3E-02	7.7E-03	6.4E-03	3.8E-03	8.1E-04	6.7E-05
					Frozen	Frozen
Average	1.22E-02	7.5E-03	6.3E-03	3.56E-03	8.27E-04	6.88E-05
St. Dev.	6.6E-05	4.5E-05	2E-05	3.8E-05	3.5E-06	4.2E-07

The above measurements indicate that our conductivity measurement is reproducible within 0.5% regardless of the conductivity cell used.

To evaluate the effect of FEC on electrolyte conductivities, we used up to six different conductivity cells for measuring electrolytes with different compositions. The range of the solvent factors in our mixture design is reported in Table 2.

Table 2. Solvent Factor ranges in Mixture Design Matrix

Components		Low		High	
Code	Name	Coded	Actual	Coded	Actual
A	EC (Ethylene Carbonate)	0	0.2	0.2	0.5
B	PC (Propylene Carbonate)	0.2	0.5	0.5	0.75
C	DMC (Dimethyl Carbonate)	0.4	0.7	0.7	0.75
D	FEC (Fluoro Ethylene Carbonate)	0	0.1	0.1	0.25

The solvent composition is subjected to the following constraint in our mixture design:
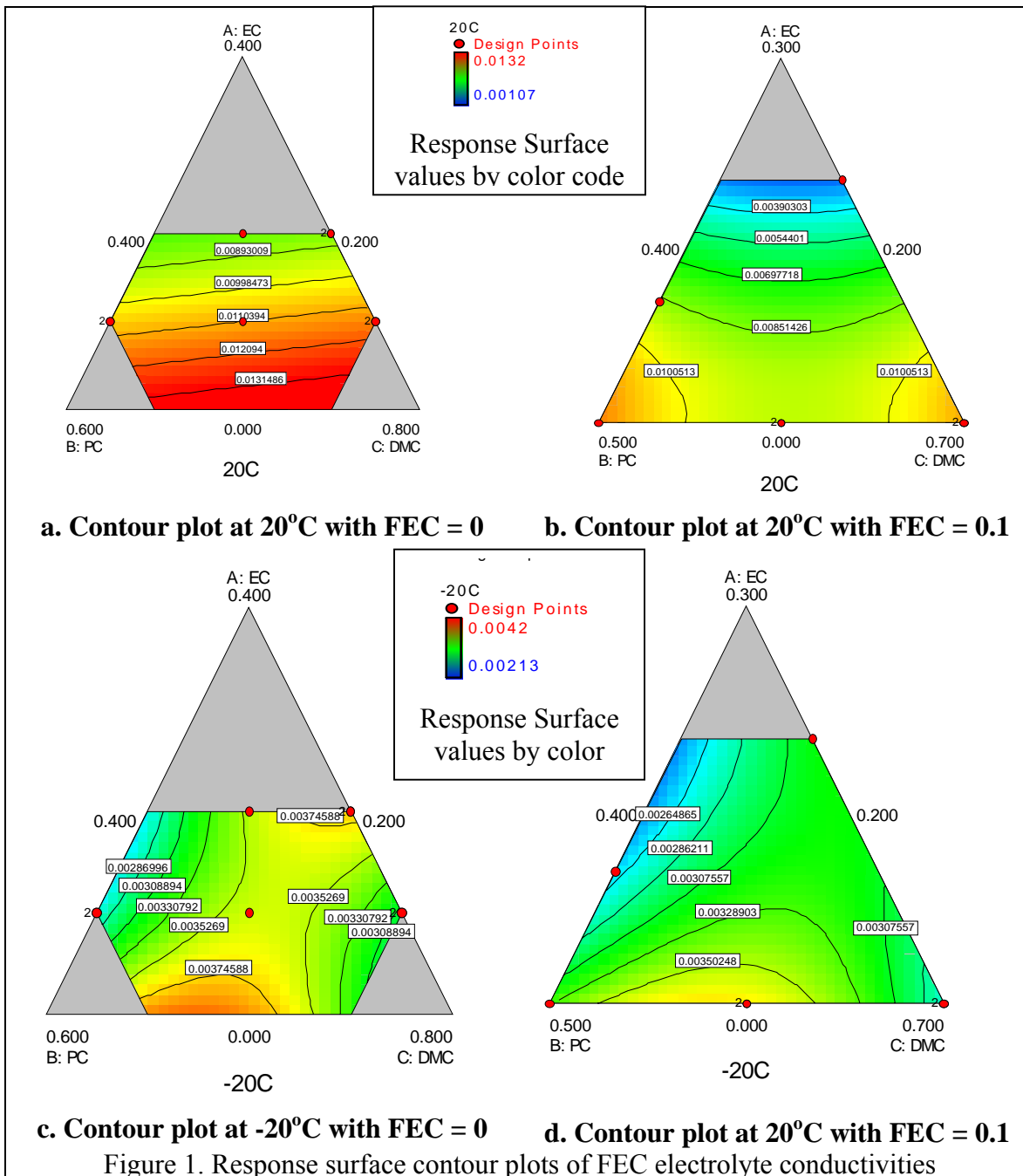
$$A + B + C + D = 1$$

The mixture design matrix and the results of the conductivity measurements at different temperatures are reported in Table 3.

Table 3. Statistical Experimental Mixture Design Matrix for FEC co-solvent

	Electrolyte Composition				20°C	0°C	-10°C	-20°C
Run	EC	PC	DMC	FEC	S/cm	S/cm	S/cm	S/cm
1	4	4	12	0	1.03E-02	6.85E-03	4.82E-03	3.76E-03
2	1	10	8	1	1.20E-02	6.68E-03	4.85E-03	3.26E-03
3	2	8	8	2	9.00E-03	5.34E-03	3.52E-03	2.71E-03
4	4	4	10	2	1.07E-02	6.36E-03	4.54E-03	3.05E-03
5	0	4	14	2	1.04E-02	6.96E-03	4.71E-03	2.80E-03
6	2	4	14	0	1.32E-02	8.18E-03	6.42E-03	2.13E-03
7	0	10	8	2	1.01E-02	6.30E-03	4.00E-03	3.17E-03
8	2.25	8.13	9.12	0.5	1.10E-02	6.73E-03	4.61E-03	3.09E-03
9	0	7	11	2	1.04E-02	6.84E-03	4.30E-03	3.43E-03
10	4	6	10	0	1.10E-02	6.33E-03	4.73E-03	3.20E-03
11	2	7	11	0	7.92E-03	5.04E-03	4.51E-03	3.97E-03
12	2	4	12	2	1.21E-02	7.06E-03	5.30E-03	3.70E-03
13	2	10	8	0	9.20E-03	5.60E-03	4.10E-03	2.83E-03
14	4	7	8	1	1.16E-02	6.51E-03	4.59E-03	3.01E-03

A Statistical Response Surface Analysis of the data was performed and contour plot of the electrolyte conductivities at 20°C and –20°C was developed. Figure 1 shows the response surface contour plot for FEC electrolyte at 20°C and –20°C.

a. Contour plot at 20°C with FEC = 0   b. Contour plot at 20°C with FEC = 0.1

c. Contour plot at -20°C with FEC = 0   d. Contour plot at 20°C with FEC = 0.1

Figure 1. Response surface contour plots of FEC electrolyte conductivities

The response surface contour plot in Fig. 1a and b indicates that, at 20°C, electrolyte conductivities increase with decreasing amounts of EC, as revealed by more reddish surface going away from the EC axis (Fig. 1a). With the presence of FEC, the conductivity of the electrolyte mixture is lower at 20°C. But at the low temperature of -20°C, there is not much difference in conductivity between electrolytes with and without FEC. However, static electrolyte properties alone (conductivity, diffusivity, viscosity, etc.) are, by themselves, insufficient to describe the effect of temperature on lithium transport from the bulk electrolyte to the electrode surface. Thus, although FEC did not significantly improve the intrinsic transport performance of a candidate electrolyte, its

virtues will reside more in how well it participates in forming compact, uniform SEI films, and how well it reduces the lithium solvation binding energy and desolvation time, and thus, how it might reduce the charge transfer resistance at the critical interfacial regions.

From this exploratory investigation, we have found that the presence of FEC <u>does indeed enhance the conductivity of the electrolyte mixture at the low temperature range</u>. Fluorinated co-solvents are not only compatible with the carbon electrodes, but they also participate in the fundamental film formation processes during initial activation and produce SEI layers with excellent characteristics for low temperature performance. Compared to the analogue non-fluorinated compounds, the fluorinated co-solvents induced lower polarization resistance at low temperature. We will compare the results of SEI film in FEC electrolyte versus the baseline electrolyte 1.2M $LiPF_6$ in EMC:EC:PC:DMC (10:20:10:60) later on.

2- INL Work on Advanced Electrolyte Model

Along with our exploratory conductivity measurements work, Dr Gering at INL has used the Advanced Electrolyte Model (AEM) tool, a theoretical approach developed at Idaho National Laboratory (INL) to screen potential electrolytes for low temperature performance. This method can yield information about five essential quantities for considering the role of transport properties and lithium de-solvation prior to cation intercalation: electrolyte conductivity, lithium transference number, lithium solvent binding energy (BE), average solvent residence time around lithium ions, and the lithium solvation number.

The INL work provides an overview of AEM-based evaluations of Li-ion electrolytes so that the role of FEC can be assessed toward optimal choices of electrolyte formulation. Upfront consideration was given to key Li-ion systems relevant to the experimental matrix of electrolyte formulations listed in EIC's mixture design of experiment, i.e., systems containing EC, PC, DMC, and FEC with $LiPF_6$ or other salts. Electrolytes based on EC/PC/DMC and $LiPF_6$ have been found to have problems with solid phase formation starting between –15 and –20 °C ([2]). Similar phase problems occur when using LiBOB, although the phase transition appears to happen at slightly lower temperatures and is formulation dependent ([3]).

Due to the thermodynamic limitations of such EC/PC/DMC systems, and in an effort to improve the overall electrolyte transport properties, systems containing gamma-butyrolactone (GBL) and/or ethyl propionate (EP) have been also modeled. Compared to traditional carbonate solvents, such ester compounds enable improved permittivity, yield comparable or improved electrolyte viscosity, while enhancing overall low-temperature operation and long term stability ([4], [5], [6]).

Dr. Gering at INL has used AEM to investigate the following electrolyte systems:

$$FEC + LiPF_6$$
$$EC + PC + DMC + LiPF_6$$
$$FEC + GBL + EP + LiPF_6$$

$$FEC + GBL + DMC + LiPF_6$$
$$FEC + EC + PC + DMC + LiPF_6$$
$$FEC + EC + GBL + DMC + LiPF_6$$
$$FEC + EC + GBL + EP + LiPF_6$$
$$FEC + EC + PC + EP + LiPF_6$$

where $LiBF_4$ is being investigated in selected systems (see discussion below).

The AEM gives accurate guidance regarding numerous transport properties, thermodynamic quantities, and solvation behavior of candidate systems. Thus, recommendations for electrolyte compositions are given based on looking at these areas at low temperature conditions. The model output is substantial, comprised of eight reports per simulation, where each simulation can consider several thousand unique conditions.

Aside from the issue of stand-alone performance of an electrolyte, the performance of the electrolyte in the cell environment is another issue, since it depends on cell chemistry and operational parameters. The consensus in the literature (covered in part by the articles listed below) generally says that FEC does affect SEI properties and can improve cyclability within cells. FEC is regarded as a beneficial cell additive in small amounts, and the overarching challenge here is deciding how much FEC should be present in the electrolyte to optimize cell performance for the EIC battery chemistry. Thus, although FEC may not significantly improve the intrinsic transport performance of a candidate electrolyte, its virtues will reside more in how it reduces the lithium solvation binding energy and desolvation time, and thus, how it might reduce the charge transfer resistance at critical interfacial regions (SEI).

AEM results indicate that FEC does indeed provide advantages regarding lithium desolvation energy and the time required for lithium desolvation, but these benefits may be minimal for electrolyte solutions with low amounts of FEC. In FEC + salt electrolytes, the AEM has determined that the activation energy required for the lithium desolvation process is lower than for carbonate-based systems, and is generally within the range of 20-35 kJ/mole, which varies over temperature and salt concentration. This activation energy quantity is based on analysis of the ion solvation component of the Li-STEP parameter within the AEM, and is related to activation energies of charge transfer resistance measured in cells containing a given electrolyte. The solvent-to-lithium binding energy for FEC determined by the AEM is generally 10-15% lower than for conventional solvents. AEM-derived ion solvation quantities at 30 °C are compared in Table 1 for the two electrolytes $EC + 1\ M\ LiPF_6$ and $FEC + 1\ M\ LiPF_6$. These modeling results underscore the advantage FEC provides in lowering the effective interaction between solvent and lithium ions.

Table 4: Comparison of key ion solvation quantities for EC and FEC-based systems at 30 °C.

System	Lithium Solvation Number	Solvent-Lithium Binding Energy (kJ/mole)	Activation Energy for lithium desolvation (kJ/mole)	Net Lithium Desolvation Time (ns)*
EC + 1 M LiPF$_6$	3.90	477.5	30.0	1.6
FEC + 1 M LiPF$_6$	3.43	426.0	24.5	1.0
Difference	-12.0%	-10.8%	-18.3%	-37.5%

* for solvated lithium at conditions listed in table. Net desolvation time is a function of temperature, solvent composition, and salt concentration.

There are other indirect benefits that arise due to the relatively weaker binding of FEC to lithium, such as the maintenance of a higher permittivity in the solvent population not directly involved in lithium solvation. Thus, the presence of FEC can act to moderate dielectric depression. Such a benefit reduces the tendency toward ion association (ion pairs and triples) and thus improves electrolyte conductivity at higher salt concentrations, which can be of greater importance under conditions of high concentration polarization within a cell.

However, regarding electrolyte transport properties (viscosity, conductivity, diffusivity, etc.), the addition of FEC does not provide a significant advantage over other additives such as chain esters or carbonates. This is due to the relatively high viscosity of pure FEC, approximately 4.1 cP at 23 °C, which for example is appreciably higher than that of PC (2.5 cP at 20 °C) and DMC (0.6 cP at 25 °C). This is an important consideration since viscosity affects most transport behavior. Moving to a *cis* or *trans*-(di)fluoro EC will drop the viscosity by nearly half, but at the penalty of decreasing the solvent permittivity by roughly one-half ([7]). This choice between fluorinated solvents could be a key issue for follow-on (Phase II) work.

These matters considered, it is generally recommended that FEC be added in amounts to promote favorable SEI characteristics, decrease the effective solvation binding energy and desolvation time of lithium, while not introducing an excessive drop in electrolyte transport performance. It appears that for many battery chemistries, 5-15% FEC in the electrolyte solvent provides a clear benefit to low-temperature cyclability.

Lastly, there is the issue of whether an alternate salt or combination of salts would provide superior performance. In studying the LiBOB salt, I have seen that its presence in electrolytes would actually counter the transport and lithium solvation benefits provided by FEC, while LiBF$_4$ would complement or enhance the virtues of FEC. The BOB$^-$ anion is less solvated than BF$_4^-$ in typical solvent systems, which translates to more solvent available to solvate lithium. Hence, BOB$^-$ adversely affects the lithium

desolvation process, yet BF_4^- aids it. This can be observed by looking at AEM-derived lithium solvation numbers and solvent-lithium binding energies: both quantities are lower in $LiBF_4$ –based electrolytes, given a solvent composition. Electrolyte viscosity is also generally lower for $LiBF_4$ electrolytes. However, it is not recommended that $LiBF_4$ be used as the sole salt in a Li-ion electrolyte due to a greater tendency for ion association to occur with this salt, which will result in a marked decrease in conductivity. Thus, a salt mixture of $LiPF_6$ and $LiBF_4$ is recommended below.

Recommended Electrolyte Formulations Based on AEM Results and Other Factors

Based on the outcome of AEM simulations performed for key systems, while considering other issues regarding cell formation, phase behavior, and long-term stability, the following list of candidate electrolyte systems are recommended (solvent proportions are by mass):

FEC + EC+ PC + DMC + $LiPF_6$ (10:20:10:60:1.2M)
FEC + EC + GBL + DMC + $LiPF_6$ (10:15:20:55:1.2M)
FEC + EC + GBL + EP + $LiPF_6$ (10:15:25:50:1.2M)
FEC + EC + GBL + EP + $LiPF_6$ + $LiBF_4$ (10:15:25:50:0.8M:0.4M)
FEC + EC + GBL+ DMC + EP + $LiPF_6$ + $LiBF_4$ (10:15:15:20:40:0.8M:0.4M)

where EMC could be a substitute for DMC in most cases. Overall, these five recommended systems should be compatible with the scope of the EIC experimental matrix, expanding it slightly with the addition of $LiBF_4$ and the ester compounds GBL and EP. The last two systems, having mixed salts, would likely be more appropriate for a Phase II effort.

Case Study: FEC + EC + GBL + EP + $LiPF_6$

This quaternary solvent electrolyte was chosen as a case study because early EIC cell test results using this electrolyte looked promising toward cycling efficiency. AEM results are given below for the particular composition of 10% FEC (by mass), 15% EC, 25% GBL, 50% EP, and variable amounts of $LiPF_6$. Figures 2-4 show AEM predictions for electrolyte viscosity, conductivity, and diffusivity, respectively, comparing the above four-solvent system to a conventional carbonate system (EC+EMC (5:5 or 1:1) + $LiPF_6$). Figure 5 shows comparative results for the Lithium Solvation and Transport Electrolyte Parameter (Li-STEP), and activation energies (E_a) of such are given in Fig. 6. Lastly, Fig. 7 compares the net time required to desolvate the lithium ion ($\Delta t_{Li+,desolv.}$) for the two electrolyte systems. Note that the Li-STEP expression is given as

$$ Li-STEP \;\; = \;\; \frac{\kappa\, t_+}{\Delta t_{Li^+,desolv.}} \left[\frac{\overline{BE}_{Li^+}}{RT} \right]^{-n_{s,Li^+}} \;\; ; \;\; \kappa\, t_+ \left[\frac{\overline{BE}_{Li^+}}{RT} \,\overline{\tau}_{Li^+} \right]^{-n_{s,Li^+}} \qquad (1) $$

where the BE term is the solvent-to-lithium binding energy averaged over all lithium solvation (coordination) numbers $n_{s,\,Li+}$, and τ_{Li+} is the average solvent residence time around lithium. This form indicates that a higher value of Li-STEP is desirable for a given temperature and composition.

Collectively, Figs. 2-7 demonstrate the benefits of choosing an electrolyte that is based both on a fluorinated additive and on intelligent selection of ester additives. The above case study is superior to the conventional electrolyte in all aspects discussed herein, yielding lower viscosity, higher conductivity and diffusivity, higher Li-STEP, lower E_a of Li-STEP, and shorter lithium desolvation times. In addition to these important issues of property screening, the other crucial test for such a candidate electrolyte is how well a secondary Li-ion battery having this electrolyte is able to cycle over various regimes of temperature, cycling rate, and cumulative test time (aging).

LSS optimizations were also performed on this case study system. The optimization parameter chosen herein is the product of electrolyte conductivity and lithium transference number ($\kappa\, t_+$). It was decided to set the concentration of FEC at 10% by mass, since this would serve as a baseline concentration for this solvent. Over one hundred different combinations of solvent proportions were involved in this study. The results of this optimization are given in Table 5, wherein solvent proportions are given that yield optimized $\kappa\, t_+$ at specified ranges of salt concentration and temperature. In general terms, the solvents having higher viscosity (EC, GBL) are at lower proportions at lower temperatures, while EP is at much higher levels. However, at higher temperatures where overall solvent permittivity is lower, the optimized concentrations of EC and GBL increase while EP decreases. It is readily seen that the above test case of 10% FEC, 15% EC, 25% GBL, and 50% EP is in good agreement with the overall LSS results.

Table 5:   Optimization results from large-scale simulations performed by AEM for the electrolyte FEC-EC-GBL-EP-LiPF$_6$, using as the optimization parameter the product of electrolyte conductivity and lithium transference number ($\kappa\, t_+$). Note that the solvent proportions are given in mass fractions, wherein the mass fraction of FEC was preset at 0.1. The results target the salt concentration range of 0.8 to 1.4 Molar.

Temperature range	FEC	EC[a]	GBL[b]	EP[d]
-30 to 0 °C	0.1	0.082	0.074 to 0.273	0.545 to 0.744
0 to 30	0.1	0.082	0.164 to 0.409	0.409 to 0.655
30 to 60	0.1	0.082 to 0.360	0.049 to 0.409[c]	0.383 to 0.614

a. When a proportion range is given, the solvent proportion is higher within that range at higher temperatures for the indicated temperature range.
b. Same as for a.
c. Trend is mixed; proportions are generally lower within the range at higher salt concentrations and are lower at higher temperatures for the indicated temperature range.
d. When a proportion range is given, the solvent proportion is lower within the range at higher temperatures for the indicated temperature range.

Conclusions

The AEM was successfully applied to novel electrolyte systems containing FEC, and insights were gained regarding the role of FEC in reducing solvent-lithium interactions,

which will potentially improve Li-ion cell cyclability. Specific ester compounds (e.g., GBL, EP) were also investigated to target improvement of Li-ion cell performance at low temperatures. An electrolyte representing a case study (FEC+EC+GBL+EP+LiPF$_6$ (10:15:25:50 (mass) + 1.2M salt)) was verified by large-scale optimization, and serves as a good Phase I candidate for exploring the proof-of-principal of such formulations. Follow-on electrolyte work (Phase II) should include more work with FEC, other fluorinated solvents (e.g., *cis* or *trans*-(di)fluoro EC) , as well as consideration of mixed salt electrolytes having LiPF$_6$ and LiBF$_4$.
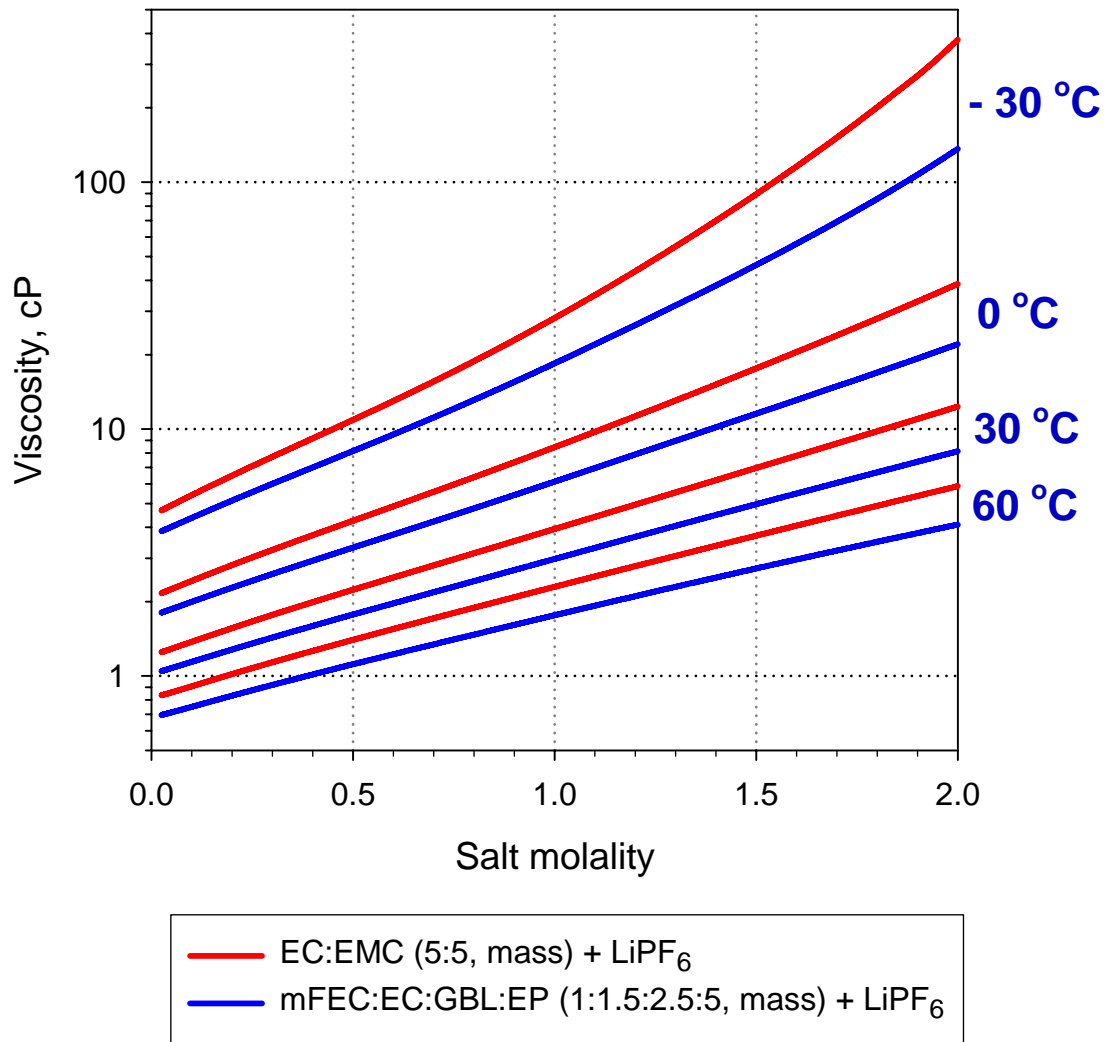
Viscosity Comparison

Fig. 2: Comparison of AEM-derived viscosity values for the conventional carbonate electrolyte versus the case study solvent system (FEC-EC-GBL-EP). The case study system is superior regarding battery electrolytes in that it exhibits lower viscosity at any chosen condition of salt concentration and temperature. Note that viscosity is shown on a log-based scale.
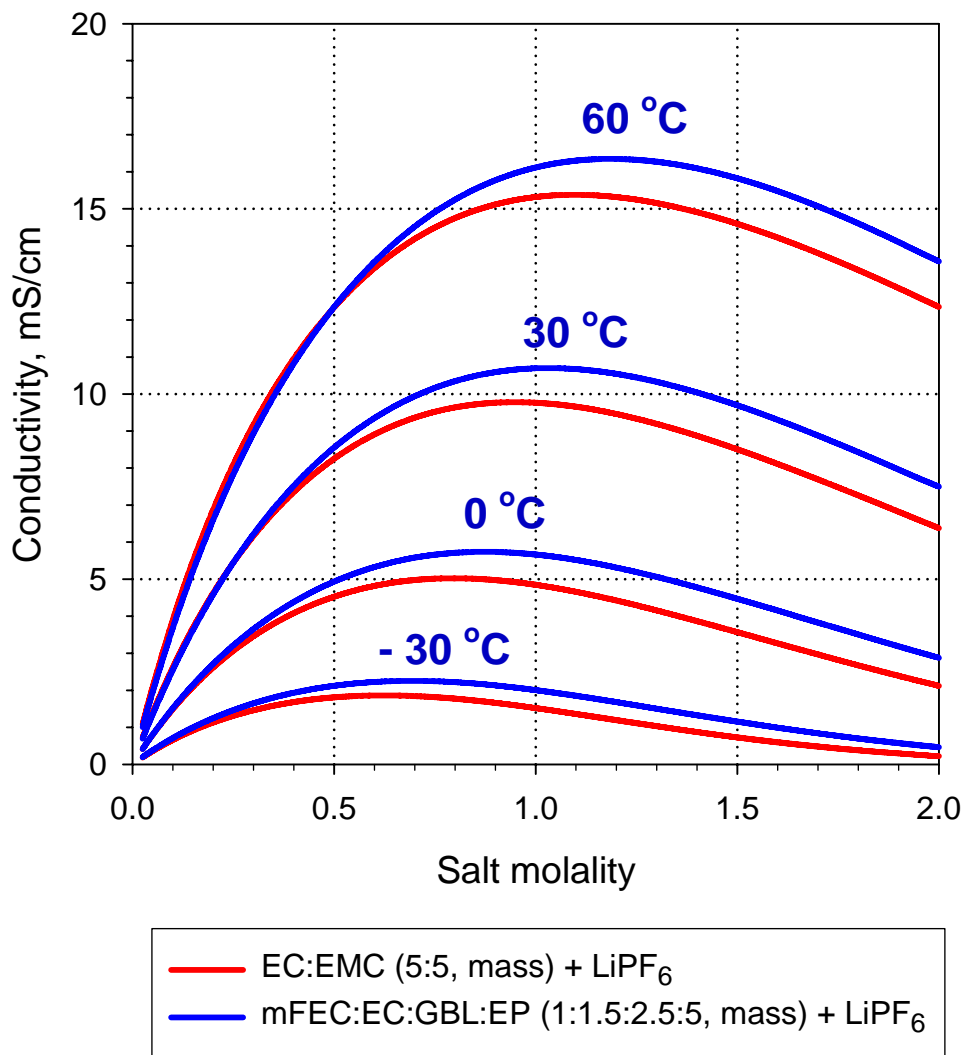
Conductivity Comparison

Fig. 3: Comparison of AEM-derived conductivity values for the conventional carbonate electrolyte versus the case study solvent system (FEC-EC-GBL-EP). The case study system is superior regarding battery electrolytes in that it exhibits higher conductivity at most conditions of salt concentration and temperature.
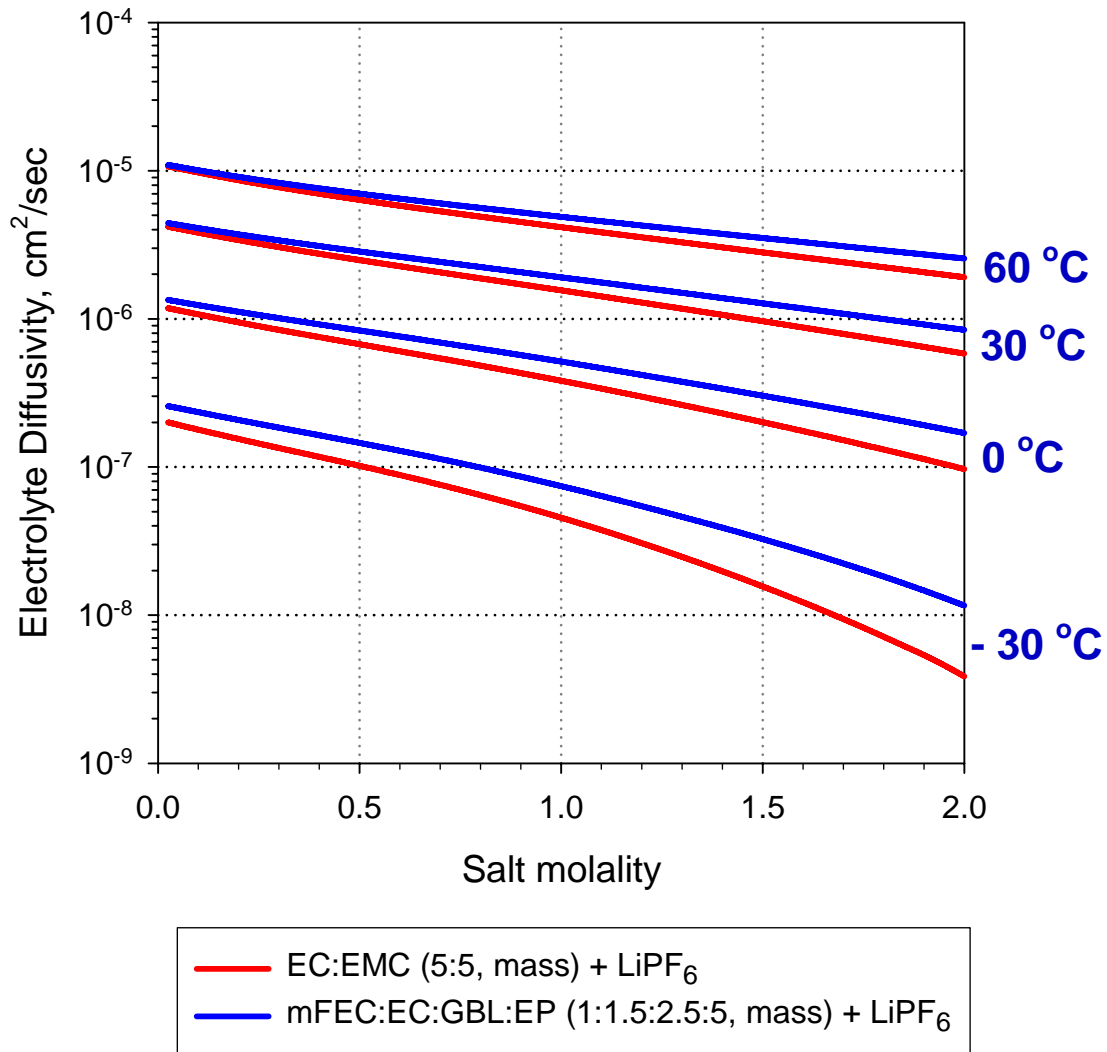
Diffusivity Comparison

Fig. 4: Comparison of AEM-derived diffusivity values for the conventional carbonate electrolyte versus the case study solvent system (FEC-EC-GBL-EP). The case study system is superior regarding battery electrolytes in that it exhibits higher diffusivity at any chosen condition of salt concentration and temperature.
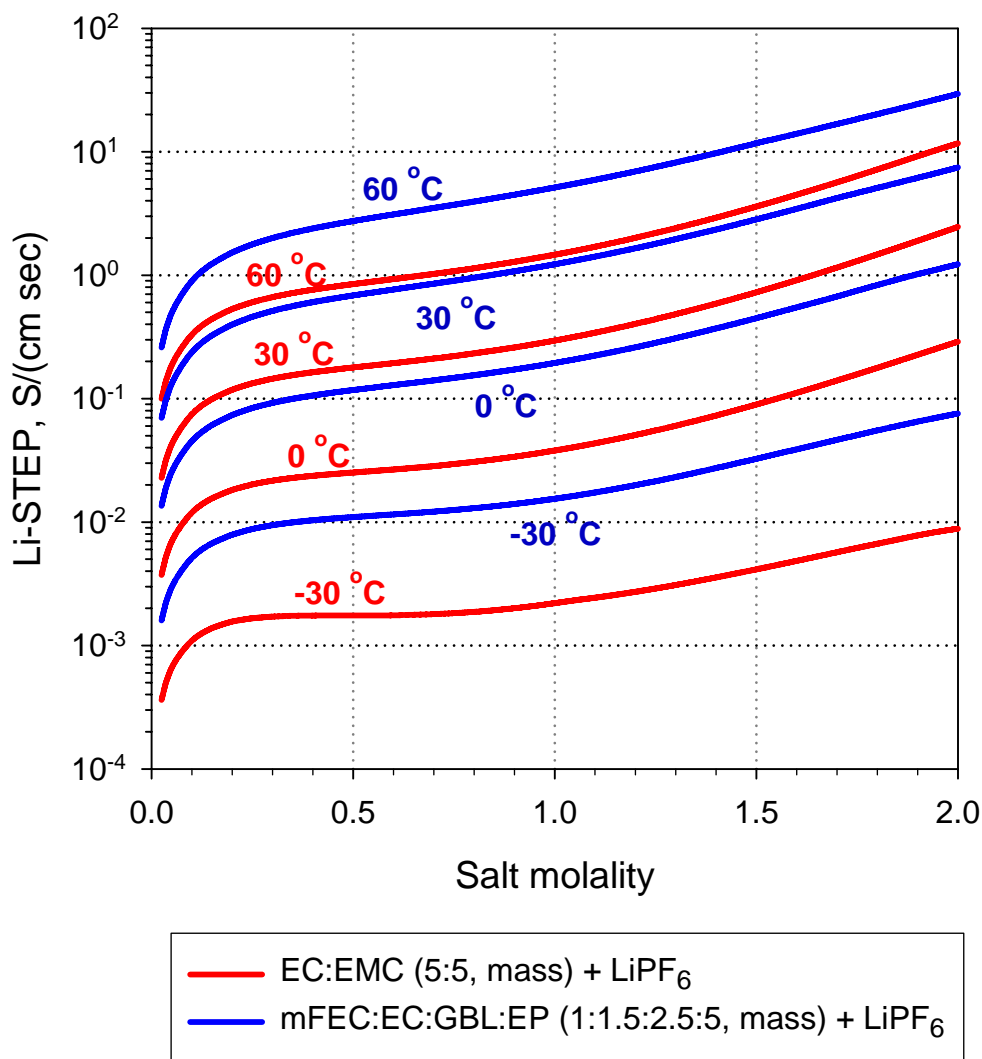
Fig. 5: Comparison of AEM-derived Li-STEP values (Eq. 1) for the conventional carbonate electrolyte versus the case study solvent system (FEC-EC-GBL-EP). The case study system is superior regarding battery electrolytes in that it exhibits higher Li-STEP at any chosen condition of salt concentration and temperature. Note that Li-STEP is shown on a log-based scale.
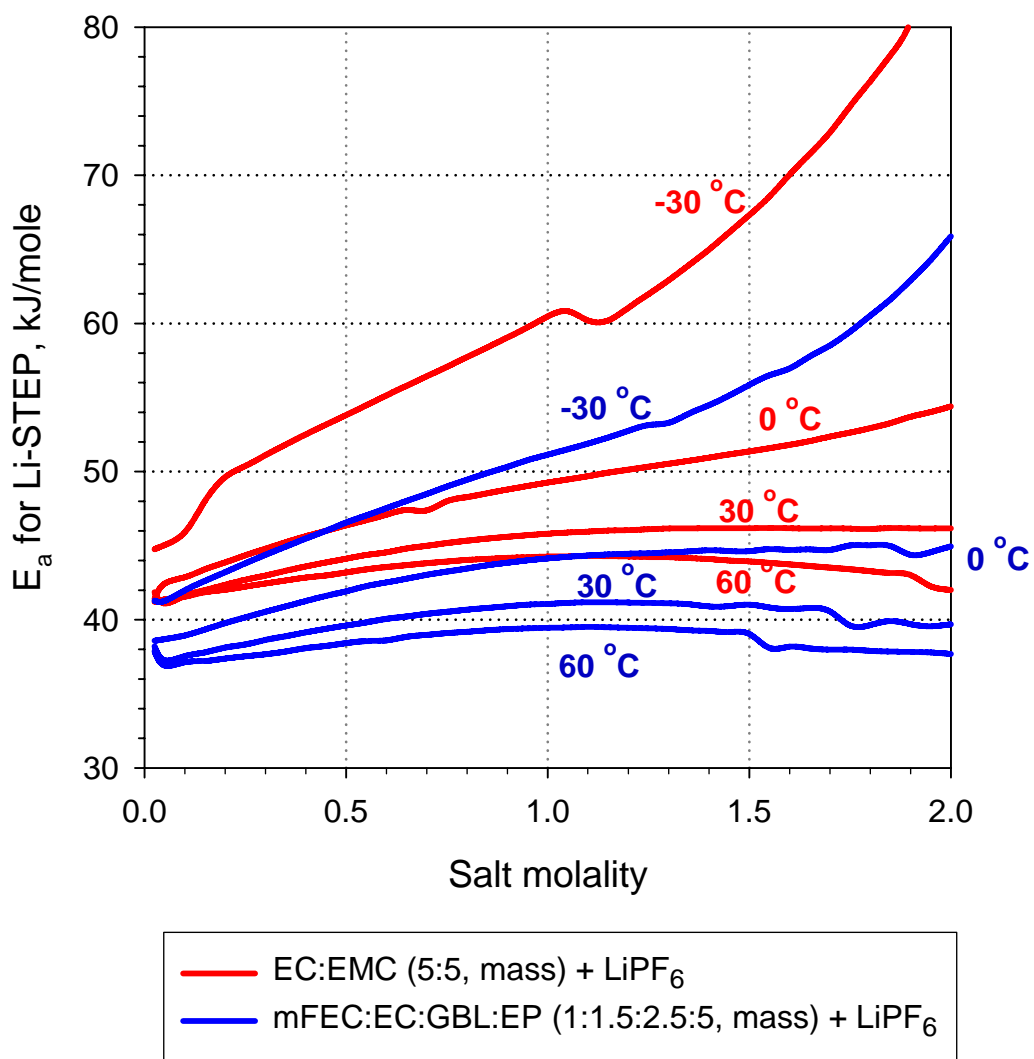
Fig. 6: Comparison of AEM-derived Li-STEP activation energies for the conventional carbonate electrolyte versus the case study solvent system (FEC-EC-GBL-EP). The case study system is superior regarding battery electrolytes in that it exhibits lower activation energies at any chosen condition of salt concentration and temperature.
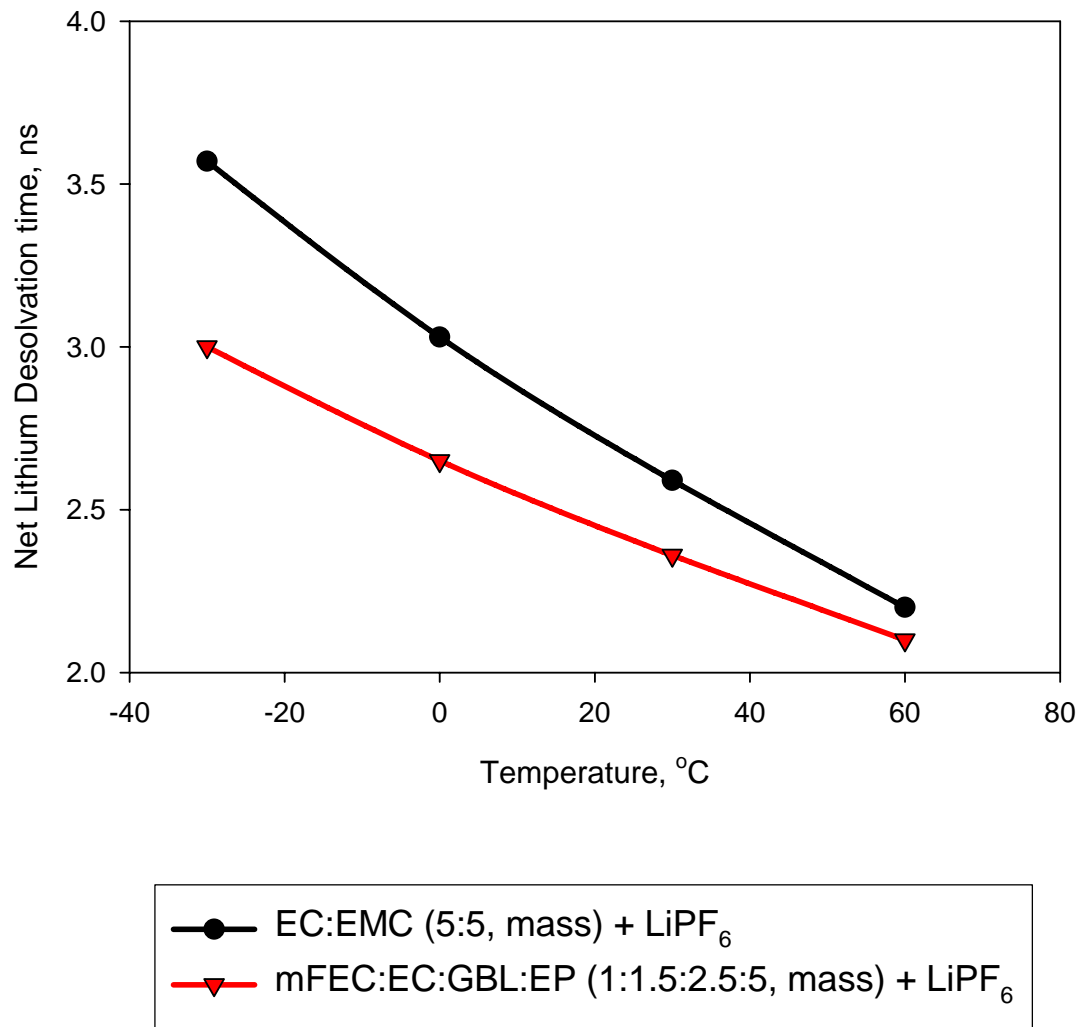
Fig. 7: Comparison of AEM-derived net lithium desolvation times for the conventional carbonate electrolyte versus the case study solvent system (FEC-EC-GBL-EP). The case study system is superior regarding battery electrolytes in that it exhibits shorter net desolvation times over the shown conditions.

3- Evaluation of SEI Film Formation on Carbon Anode and Doped Cathode Materials

The fundamental problem of poor low temperature performance is related to the interfacial impedance at the electrodes. Our goal in this Phase I program is to develop new electrolyte formulation that would form SEI film with low interfacial impedance on different anode and cathode materials. Low cell impedance at low temperatures will translate into high power for cold cranking and high Regen charge.

We use electrochemical impedance spectroscopy (EIS) to measure the interfacial impedance of different carbon and cathode materials in half-cells (i.e. Li/Carbon cell and Li/Cathode) as well as in full cell configurations at two different temperatures, 20°C and –20°C. Impedance is a non-destructive technique that provides useful information about charge transport in the bulk and charge transfer across interfaces. The relative change of impedance is extremely useful in assessing the stability of interfaces.

Since Li anode is used in the half-cells, the difference in the impedance spectra obtained will be directly correlated to the different carbon/graphite materials. Literature studies suggest that the poor performance of Li-ion batteries at low temperature is much more severe than that can be predicted from the relationship between electrolyte conductivity and temperature ([1]). Furthermore, it has been recognized that the performance of Li-ion cells is dependent on the nature of the passive film formed on the electrode surfaces ([8]). On the anode, the film formation is the result of electrolyte reduction on the surface during the initial formation cycles. The role of this surface layer interface is critical to the working of carbon electrode. This so-called solid electrolyte interface (SEI) is both a conductor for lithium ions and an electronic insulator, and it prevents further electrolyte decomposition on the carbon surface. The SEI films also exist on the cathode but they are thinner ([9]), suggesting the irreversible capacity loss due to SEI film formation on the cathodes is less than for graphite anodes. At low temperature, polarization on the anode becomes quite large and it is much more severe than at the metal oxide cathode.

To determine the cell component that is most influenced by the temperature change, we have studied the impedance of a Li-ion cell as a function of temperatures using the Electrochemical Impedance Spectra (EIS) technique. The main resistance components in the charge/discharge kinetics of Li-ion cells are:

Ohmic resistance: Migration and transport of ions from the bulk electrolytes to the active electrodes

Interfacial Resistance: De-solvation of Li ion near the SEI/electrolyte interface and diffusion of Li-ion through the SEI layer to the active electrode surface

Diffusion resistance: Insertion of Li-ion into the interstitial sites of the host lattice, either the oxide cathode or carbon anode

These resistance components can be separated by EIS using an equivalent circuit analysis. In our analysis, we have used the following circuit for fitting our measured data
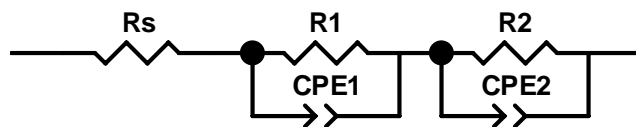
Figure 8. Equivalent circuit for SEI film in Li-ion cell

where Rs is the Ohmic resistance, R_1 the interfacial resistance, R_2 the diffusion resistance and the CPEs are the constant phase elements. To determine the value of the various resistances, we ran the simulation data option and changed the values of all the components until we find a good fit for the experimental data.

 We measured the SEI film resistance in the following five electrolytes:

FEC + EC+ PC + DMC + $LiPF_6$ (10:20:10:60:1.2M)
FEC + EC + GBL + DMC + $LiPF_6$ (10:15:20:55:1.2M)
FEC + EC + GBL + EP + $LiPF_6$ (10:15:25:50:1.2M)
FEC + EC + GBL + EP + $LiPF_6$ + $LiBF_4$ (10:15:25:50:0.8M:0.4M)
EMC+EC + PC + DMC + $LiPF_6$ (10:20:10:60:1.2M)

3.1 Cell Construction

We used both Half-cells with Li anode and full cells for evaluating the SEI film formed in different electrolytes. The theoretical capacities of cells are about 50mAh. The cells are sandwiched between two plates during cycling so that to maintain uniform pressure between cells (Fig. 8). EIS results are sensitive to the pressure applied to the cell stack. By applying standard even pressure to all cells during EIS measurements and cycling, we can reduce extraneous error and the results will reveal the true differences in performance between the electrolytes. All the cells are cycled for five times before EIS measurements are performed.

	Electrode Dimensions: 1" x 1.75" Li thickness: 7 mils Electrode thickness: 5-8 mils Electrode loading: 4 mAh/cm^2 Separator: Celgard 3401 Pouch material: Heat sealable foil/poly bag
Figure 8. Test cell set-up and dimensions	

AC impedance measurements were performed with a Solartron SI 1287 electrochemical interface and an SI 1260 impedance/gain-phase analyzer using CorrWare and Zplot software. The impedance data were analyzed with Zview software.

3.2 SEI Resistance Components for Anode Materials

 We have evaluated the following anode materials:

- MCMB

- Superior Graphite G1520P

- Superior Graphite G1520M

MesoCarbon MicroBeads (MCMB) were used as a benchmark anode material to compare with two graphite materials that we obtained from Superior Graphite. MCMB is the standard anode material for Li-ion batteries, with a reversible capacity of 300-340 mAh and excellent cyclability. MCMB consists of many small graphite particles with spherical shape.

Superior Graphite consists of high purity flake graphite chemically treated on the surface so that a thin amorphous carbon layer is formed. The two standard grades available are Superior Graphite 1520M and 1520P for this application. The 1520P has been specially treated to be PC resistant. Except for the difference in surface treatments, the physical properties of the two are practically the same. The particle size distribution and SEM pictures of both Superior Graphite anode materials are shown in Figure 9.
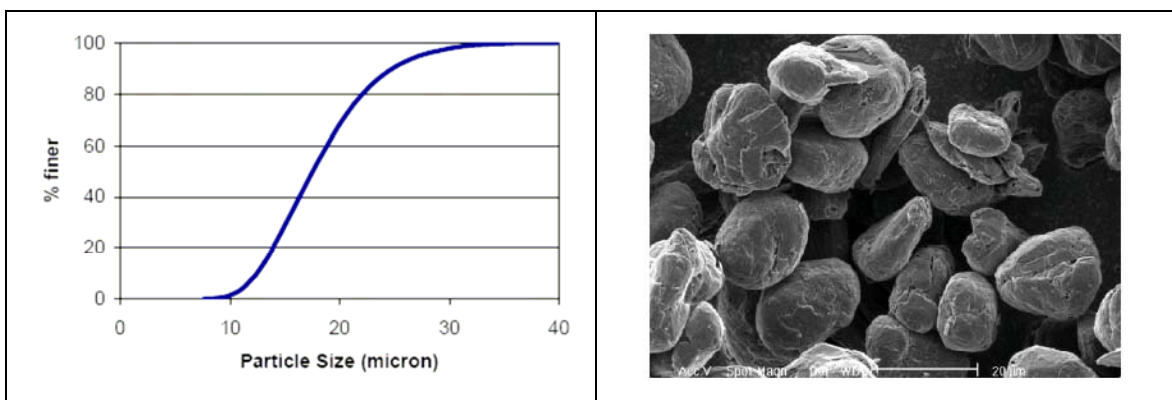

Figure 9. Particle size distribution and SEM of Superior Graphite materials

3.2.1 AC Impedance Analysis of Li/MCMB Half Cells

The SEI film resistance for the MCMB anode in a half-cell configuration is reported in Figure 10. AC impedance measurements were taken with the cells in the fully discharged state.

Figure

Figure 10. SEI film resistance for Li/MCMB half cell in different electrolytes
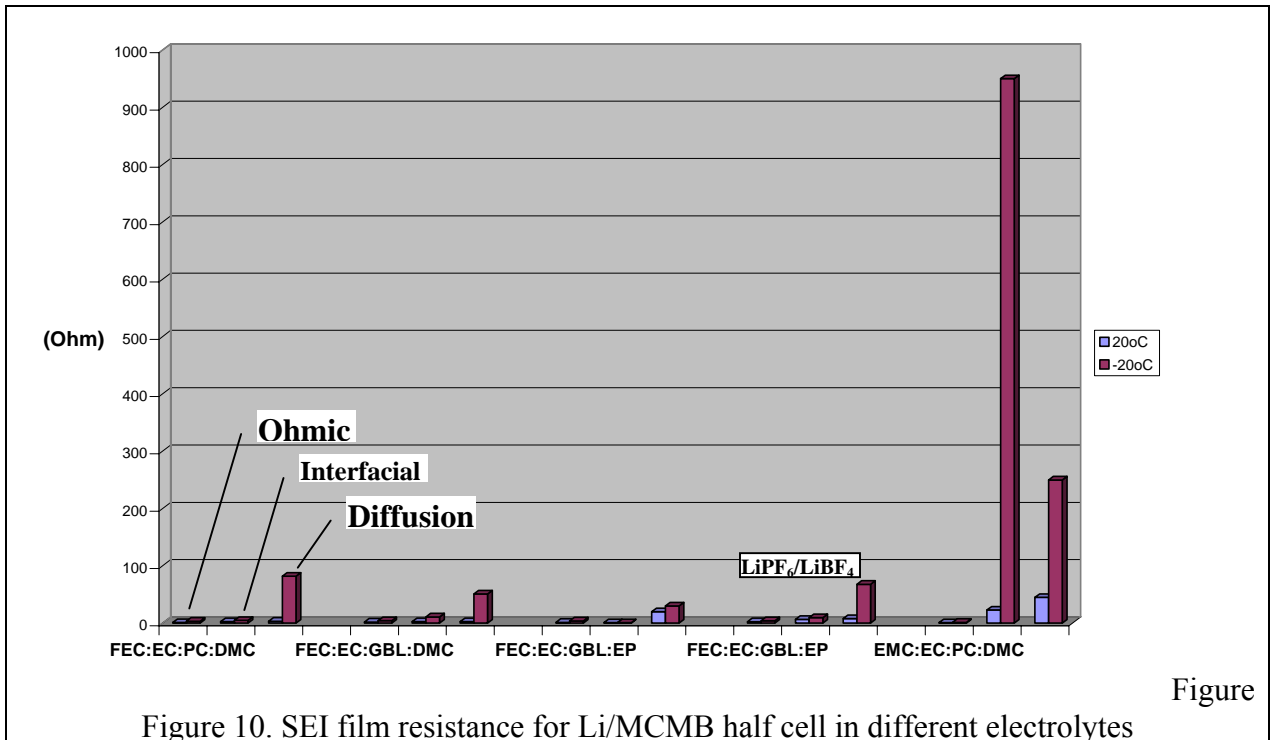
The results obtained with FEC electrolytes are quite consistent and revealing. The SEI impedance spectra and the simulation results for MCMB anode are reported in Figures 11 to 15. Figure 10 indicates that the SEI film resistances of Li/MCMB half cells with the FEC electrolyte are much lower than that of the baseline EMC:EC:PC:DMC electrolyte. For example, the interfacial resistances for FEC:EC:GBL:EP are respectively 0.9Ω at both 20°C and -20°C (Fig. 13). For the baseline electrolyte EC:EMC:PC:DMC, the interfacial resistances are respectively 23Ω and 950 Ω at 20°C and -20°C. The very overwhelming low SEI film impedance for FEC electrolyte will translate into high power for cold cranking and high Regen charge.

Figure 11. Li/MCMB w/ 10% C in 1.2M LiPF6 FEC:EC:PC:DMC (10:20:10:60)

Discharge; Impedance at RT	Discharge; Impedance at -20°C
Ohmic Resistance: 1.2 Interfacial Resistance: 2.7 Diffusion Resistance: 3.5	Ohmic Resistance: 3.5 Interfacial Resistance: 4.7 Diffusion Resistance: 82
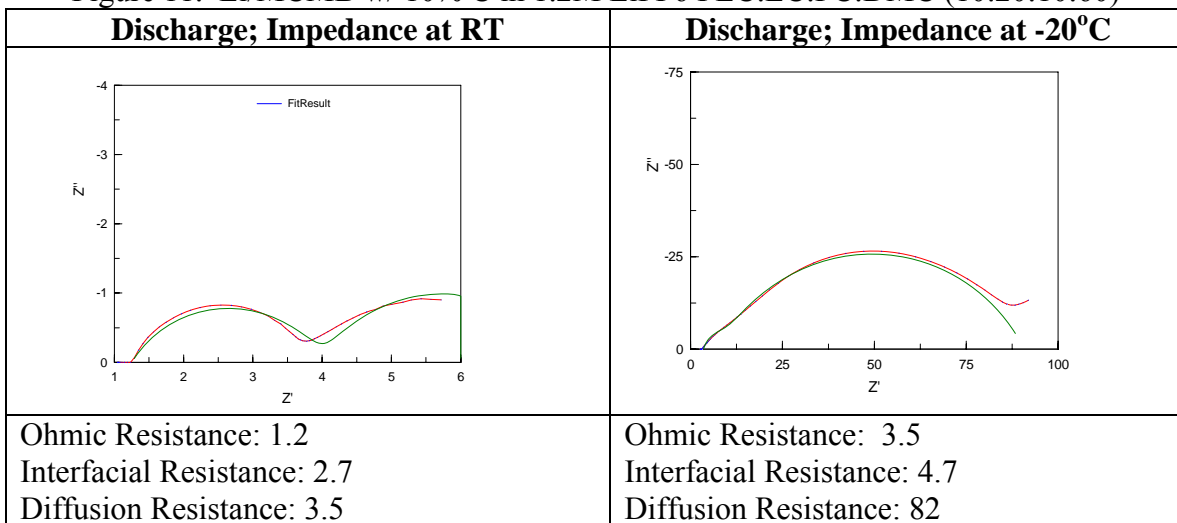
Figure 12. Li/MCMB w/ 10% C in 1.2M LiPF6 FEC:EC:GBL:DMC (10:15:20:55)

Discharge; Impedance at RT	Discharge; Impedance at -20°C
Ohmic Resistance: 2.1 Interfacial Resistance: 2.6 Diffusion Resistance: 2.7	Ohmic Resistance: 4.5 Interfacial Resistance: 11 Diffusion Resistance: 51
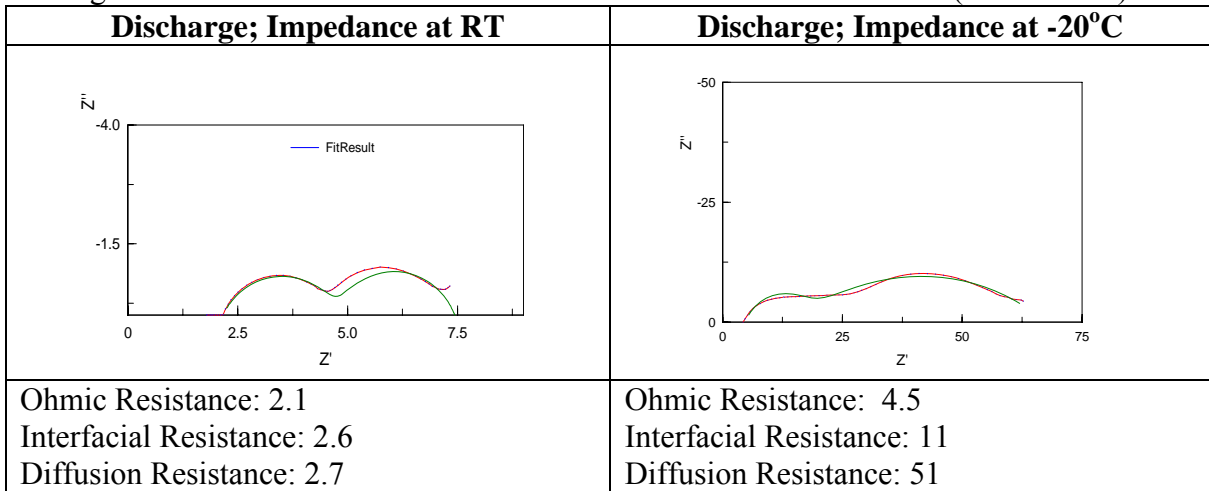
Figure 13. Li/MCMB w/ 1.2M LiPF$_6$ in FEC:EC:GBL:EP (10:15:25:50)

Discharge; Impedance at at RT	Discharge; Impedance at -20°C
Ohmic Resistance: 1.4 Interfacial Resistance: 0.9 Diffusion Resistance: 20	Ohmic Resistance: 3.8 Interfacial Resistance: 0.9 Diffusion Resistance: 30
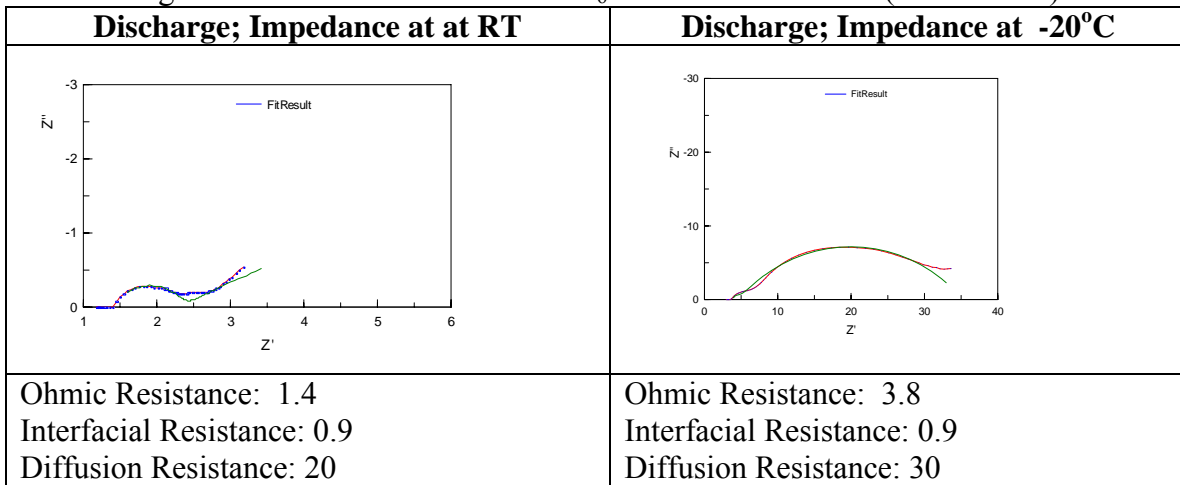
Figure 14. Li/MCMB w/ 0.8M LiPF$_6$+0/4M LiBF$_4$ in FEC:EC:GBL:EP (10:15:25:50)

Discharge; Impedance at at RT	Discharge; Impedance at -20°C
Ohmic Resistance: 2.4 Interfacial Resistance: 6.5 Diffusion Resistance: 8	Ohmic Resistance: 4.2 Interfacial Resistance: 9.7 Diffusion Resistance: 68
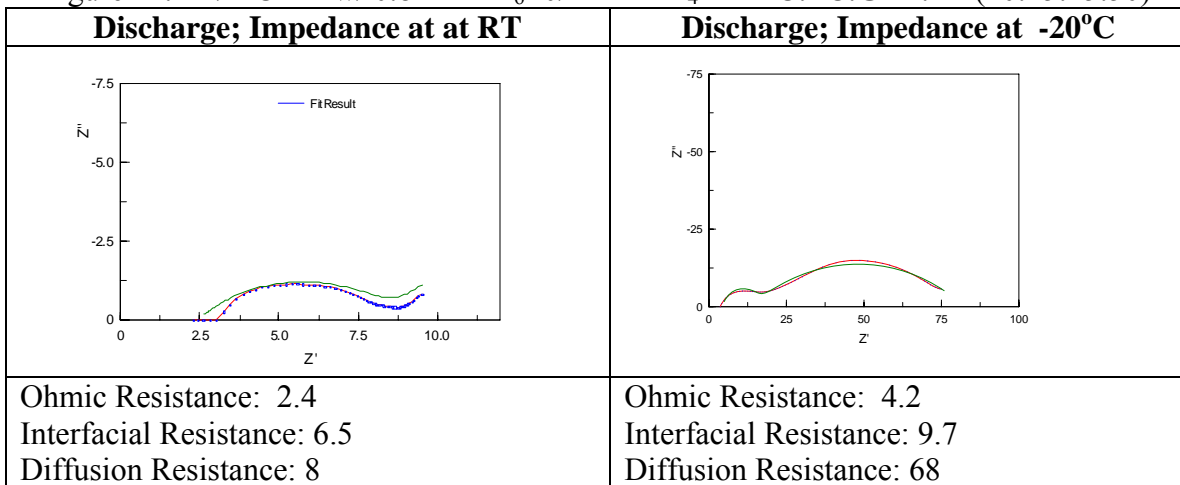
Figure 15. Li/MCMB w/ 1.2M LiPF$_6$ EMC:EC:PC:DMC (10:20:10:60)

Discharge; Impedance at at RT	Discharge; Impedance at -20°C
Ohmic Resistance: 0.8 Interfacial Resistance: 23 Diffusion Resistance: 45	Ohmic Resistance: 1.3 Interfacial Resistance: 950 Diffusion Resistance: 250
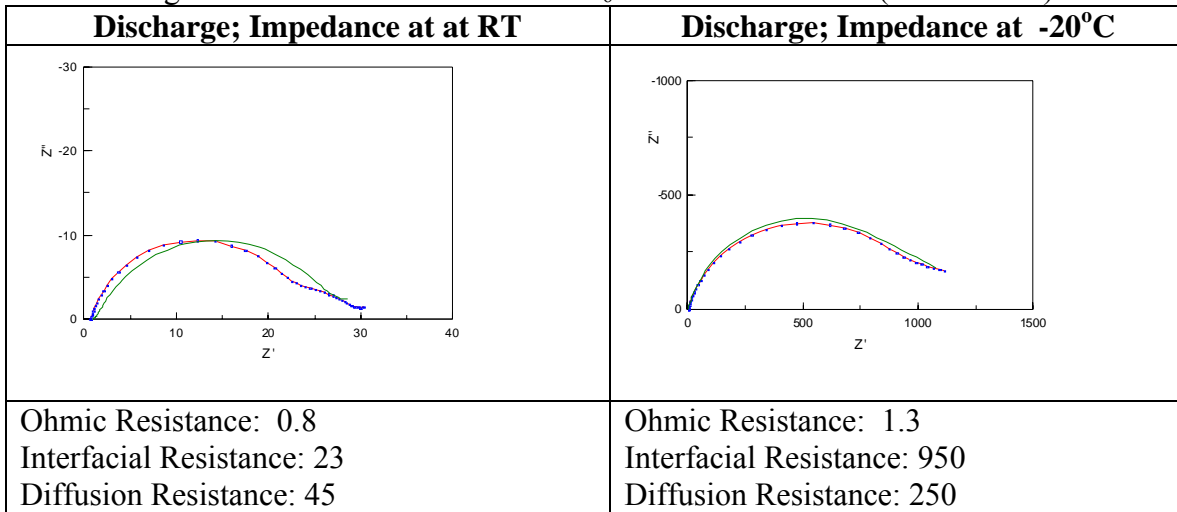
3.2.2 AC Impedance Analysis of Li/SG1520P Half Cells

The SEI film resistance for the MCMB anode in the half-cell configuration is reported in Figure 16. AC impedance measurements were taken with the cells in the fully discharge state.
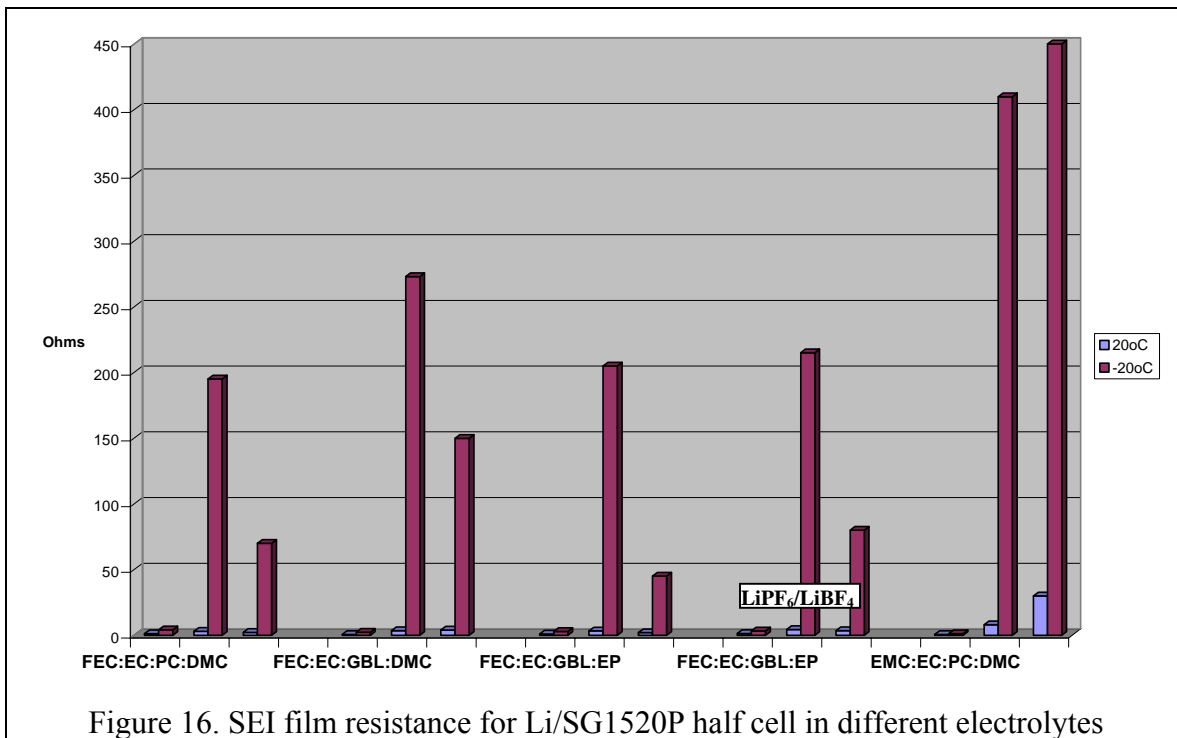
Figure 16. SEI film resistance for Li/SG1520P half cell in different electrolytes

The SEI impedance spectra and the simulation results for the SG1520P anode are reported in Figures 17 to 21. For these Superior Graphite materials, the SEI film impedance values in FEC electrolytes at -20°C were consistently lower than that of the baseline electrolyte. However, they were not as dramatic as with MCMB anode material.

Figure17. Li/SG1520P w/ 10% C in 1.2M LiPF$_6$ FEC:EC:PC:DMC (10:20:10:60)

| Discharge; Impedance at RT	Discharge; Impedance at -20°C
Ohmic Resistance: 1.2 Interfacial Resistance: 3 Diffusion Resistance: 2.1	Ohmic Resistance: 4.2 Interfacial Resistance: 195 Diffusion Resistance: 70
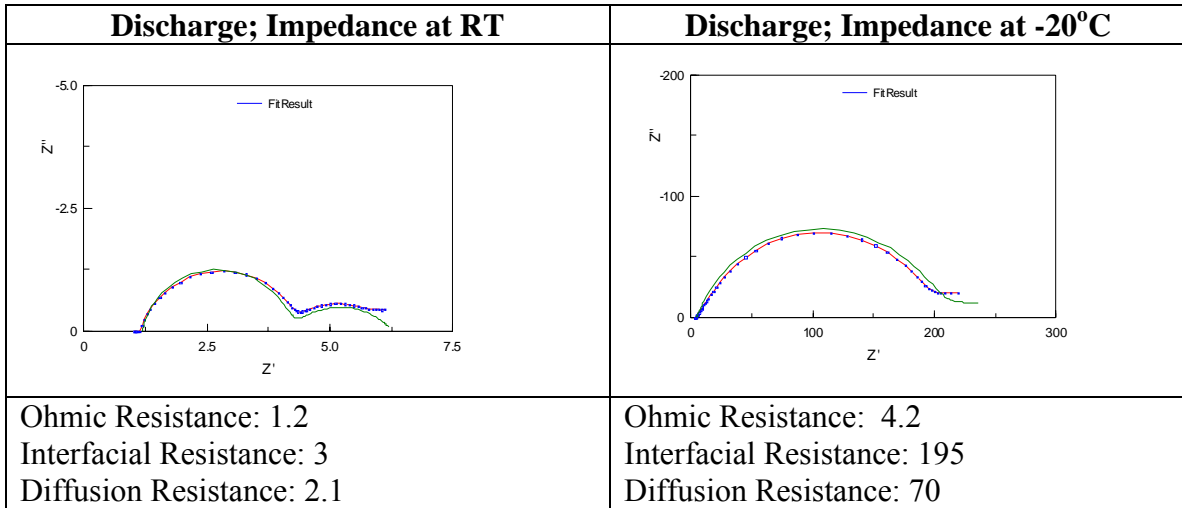
Figure 18. Li/SG1520P w/ 10% C in 1.2M LiPF$_6$ FEC:EC:GBL:DMC (10:15:20:55)

Discharge; Impedance at RT	Discharge; Impedance at -20°C
Ohmic Resistance: 0.6 Interfacial Resistance: 3.5 Diffusion Resistance: 4	Ohmic Resistance: 2.3 Interfacial Resistance: 273 Diffusion Resistance: 150
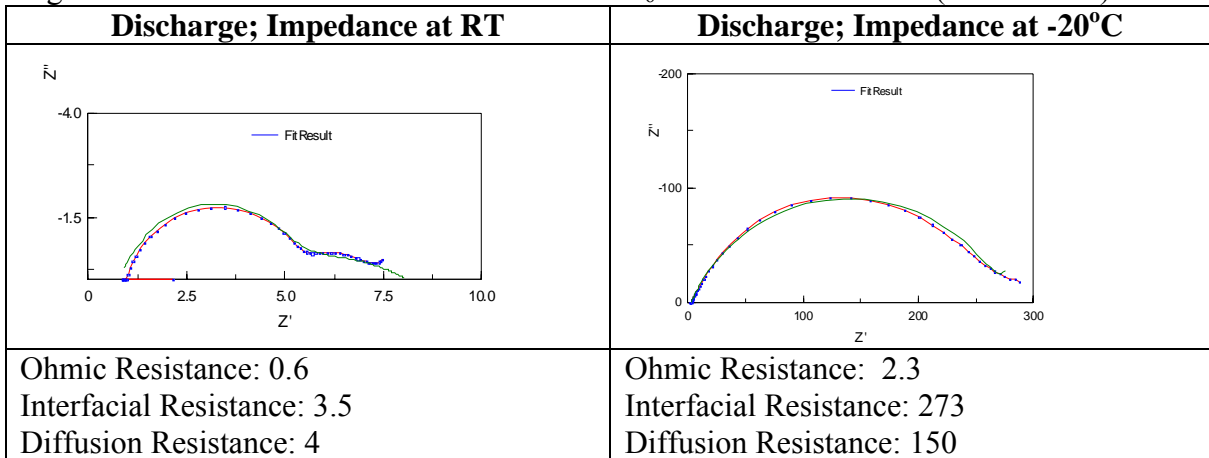
Figure 19. Li/SG1520P w/ 1.2M LiPF6 in FEC:EC:GBL:EP (10:15:25:50)

Discharge; Impedance at at RT	Discharge; Impedance at -20°C
Ohmic Resistance: 0.9 Interfacial Resistance: 3.3 Diffusion Resistance: 2	Ohmic Resistance: 2.9 Interfacial Resistance: 205 Diffusion Resistance: 45
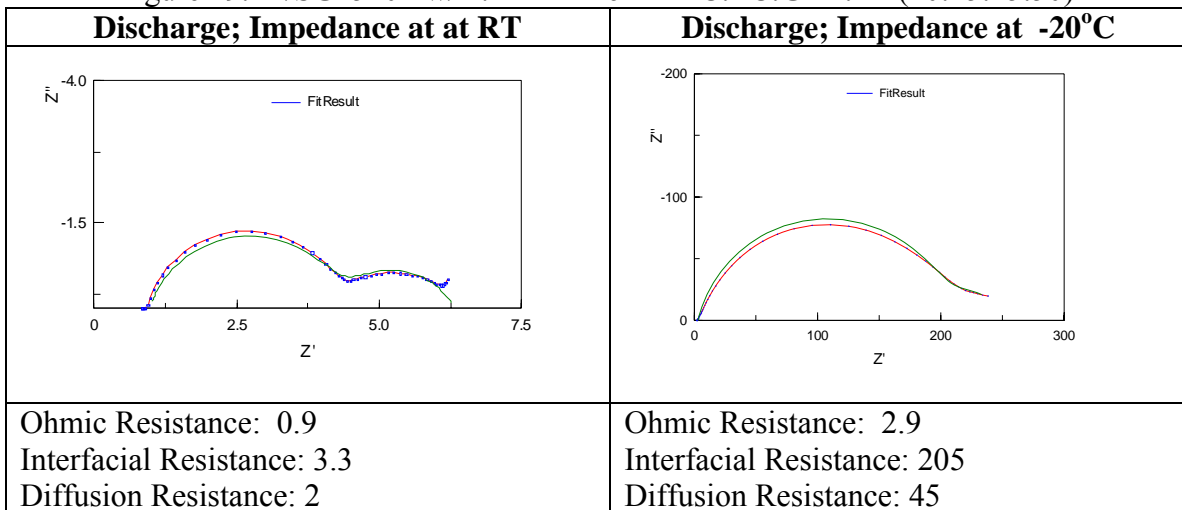
Figure 20. Li/SG1520P w/ 0.8M LiPF$_6$+0/4M LiBF$_4$ in FEC:EC:GBL:EP (10:15:25:50)

Discharge; Impedance at at RT	Discharge; Impedance at -20°C
Ohmic Resistance: 1.3 Interfacial Resistance: 4.3 Diffusion Resistance: 3.5	Ohmic Resistance: 3.2 Interfacial Resistance: 215 Diffusion Resistance: 80
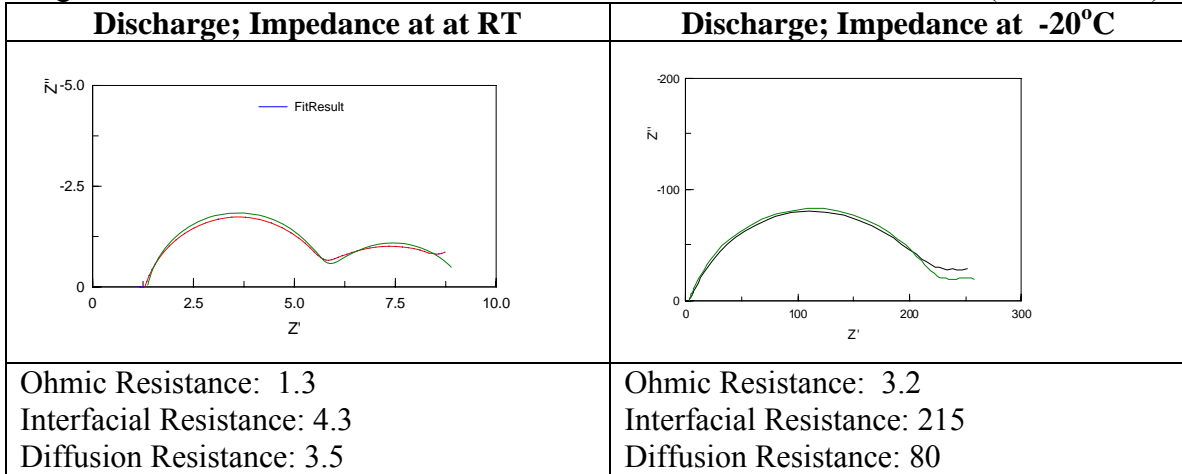
Figure 21. Li/SG1520P w/ 1.2M LiPF$_6$ EMC:EC:PC:DMC (10:20:10:60)

Discharge; Impedance at at RT	Discharge; Impedance at -20°C
Ohmic Resistance: 0.6 Interfacial Resistance: 8 Diffusion Resistance: 30	Ohmic Resistance: 1.2 Interfacial Resistance: 410 Diffusion Resistance: 450
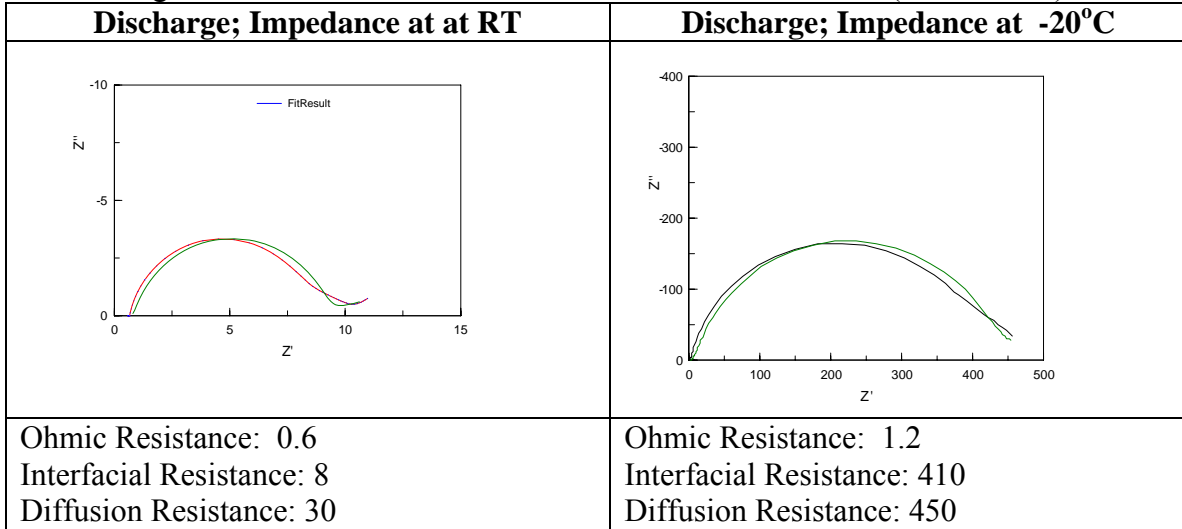
3.2.3 AC Impedance Analysis of Li/SG1520M Half Cells

The SEI film resistance for the SG1520M anode in the half-cell configuration is reported in Figure 16. AC impedance measurements were taken with the cells in the fully discharge state.

Figure 16. SEI film resistance for Li/SG1520M half cell in different electrolytes
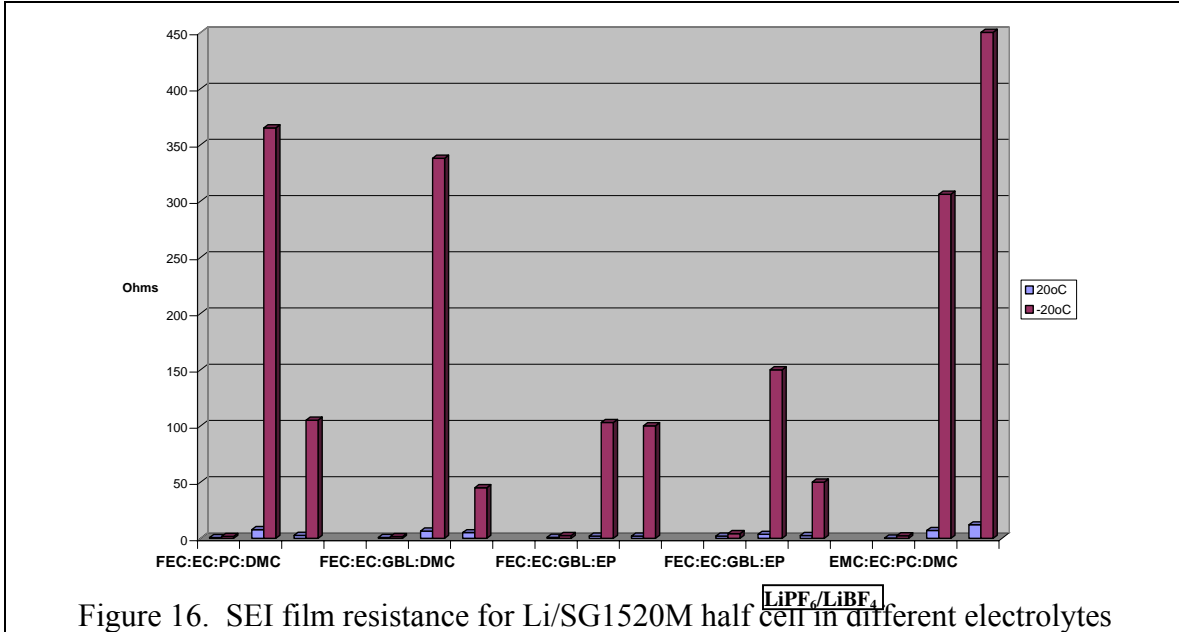
The SEI impedance spectra and the simulation results for SG1520M anode are reported in Figures 17 to 21. For the Superior Graphite SG1520M material, the SEI film impedance values in FEC electrolytes at -20°C were consistently lower than that of the baseline electrolyte. FEC electrolytes containing GBL/EP had significantly lower SEI film impedance at the low temperature range. However, as with the SG1520P, they were not as low as with MCMB anode material.

Figure 17. Li/SG1520M w/ 10% C in 1.2M LiPF$_6$ FEC:EC:PC:DMC (10:20:10:60)

Discharge; Impedance at RT	Discharge; Impedance at -20°C
Ohmic Resistance: 0.65 Interfacial Resistance: 7.7 Diffusion Resistance: 2.6	Ohmic Resistance: 1.6 Interfacial Resistance: 365 Diffusion Resistance: 105

Figure 18. Li/SG1520M w/ 10% C in 1.2M LiPF$_6$ FEC:EC:GBL:DMC (10:15:20:55)

Discharge; Impedance at RT	Discharge; Impedance at -20°C
Ohmic Resistance: 0.8 Interfacial Resistance: 6.5 Diffusion Resistance: 5	Ohmic Resistance: 1.5 Interfacial Resistance: 337 Diffusion Resistance: 45

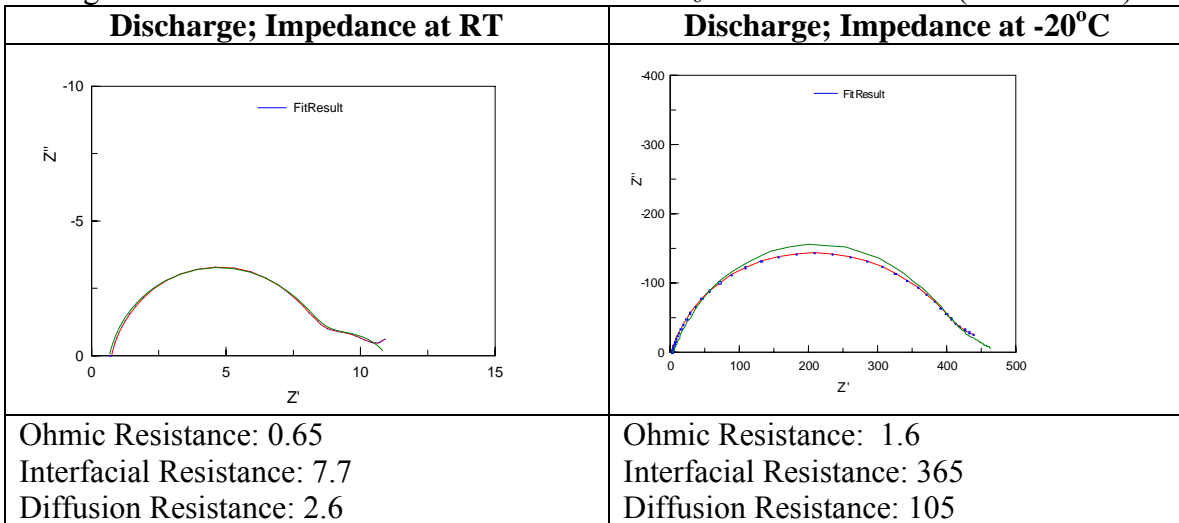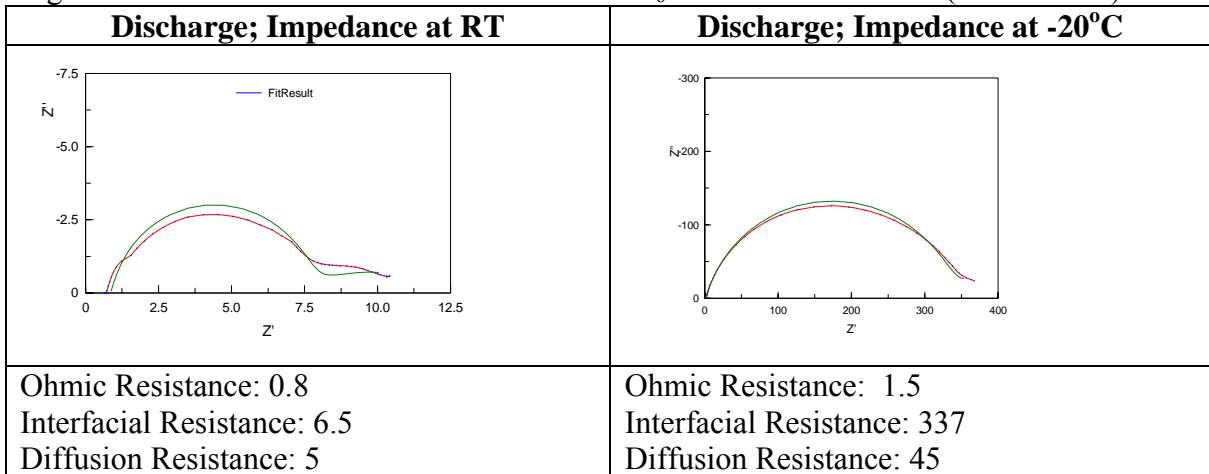Figure 19. Li/SG1520M w/ 1.2M LiPF$_6$ in FEC:EC:GBL:EP (10:15:25:50)

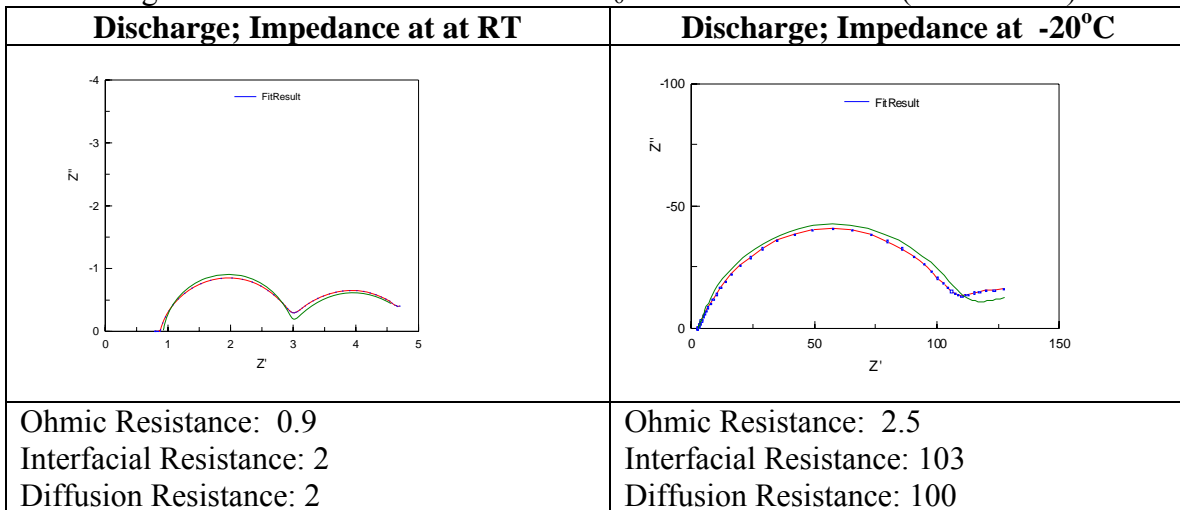| Discharge; Impedance at at RT	Discharge; Impedance at -20°C
Ohmic Resistance: 0.9 Interfacial Resistance: 2 Diffusion Resistance: 2	Ohmic Resistance: 2.5 Interfacial Resistance: 103 Diffusion Resistance: 100

Figure 20. Li/SG1520M w/ 0.8M LiPF$_6$+0/4M LiBF$_4$ in FEC:EC:GBL:EP (10:15:25:50)

Discharge; Impedance at at RT	Discharge; Impedance at -20°C
Ohmic Resistance: 1.9 Interfacial Resistance: 3.5 Diffusion Resistance: 2.5	Ohmic Resistance: 4.2 Interfacial Resistance: 150 Diffusion Resistance: 50
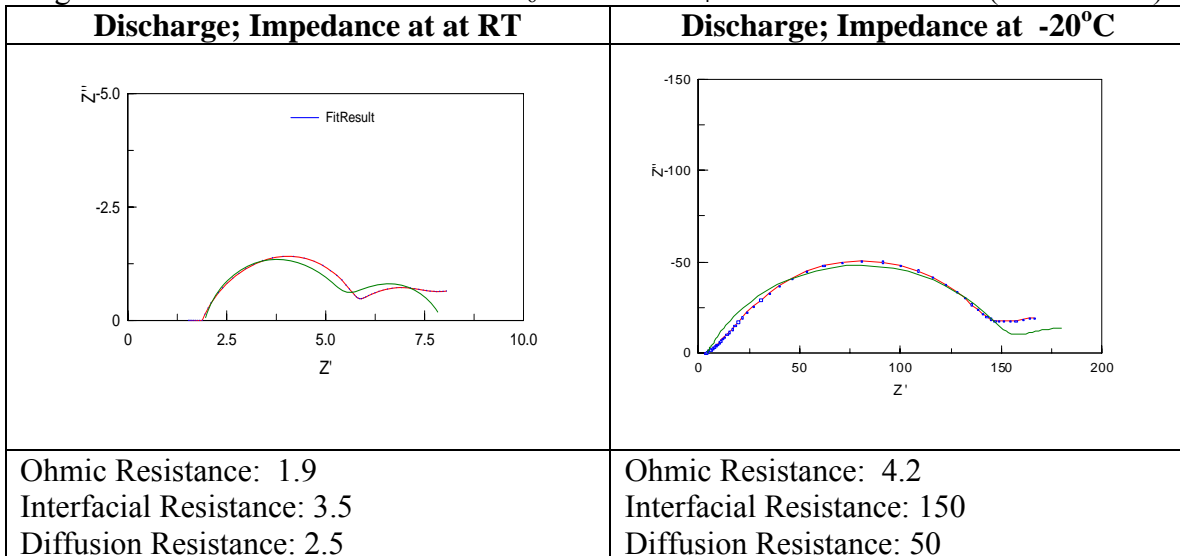
Figure 21. Li/SG1520M w/ 1.2M LiPF$_6$ EMC:EC:PC:DMC (10:20:10:60)

Discharge; Impedance at at RT	Discharge; Impedance at -20°C
Ohmic Resistance: 0.2 Interfacial Resistance: 7 Diffusion Resistance: 12	Ohmic Resistance: 2.2 Interfacial Resistance: 306 Diffusion Resistance: 450
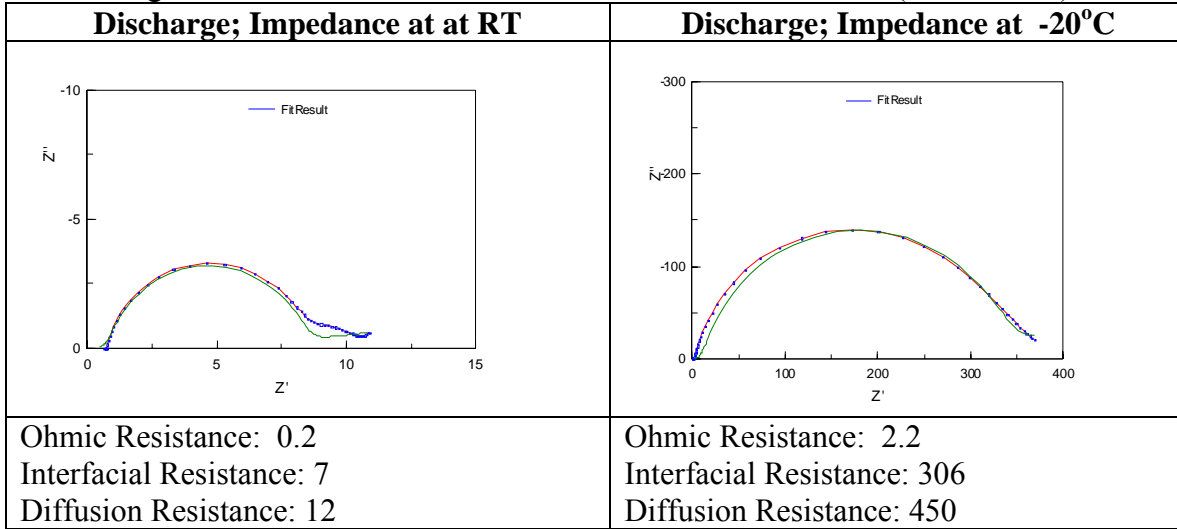
3.2.4 <u>AC Impedance Analysis of Al-Doped LiMn$_2$O$_4$ Cathode Material</u>

The SEI film resistance for Al-doped LiMn$_2$O$_4$ cathode in half-cell configuration is reported in Figure 22. AC impedance measurements were taken with the cells in fully charge state.
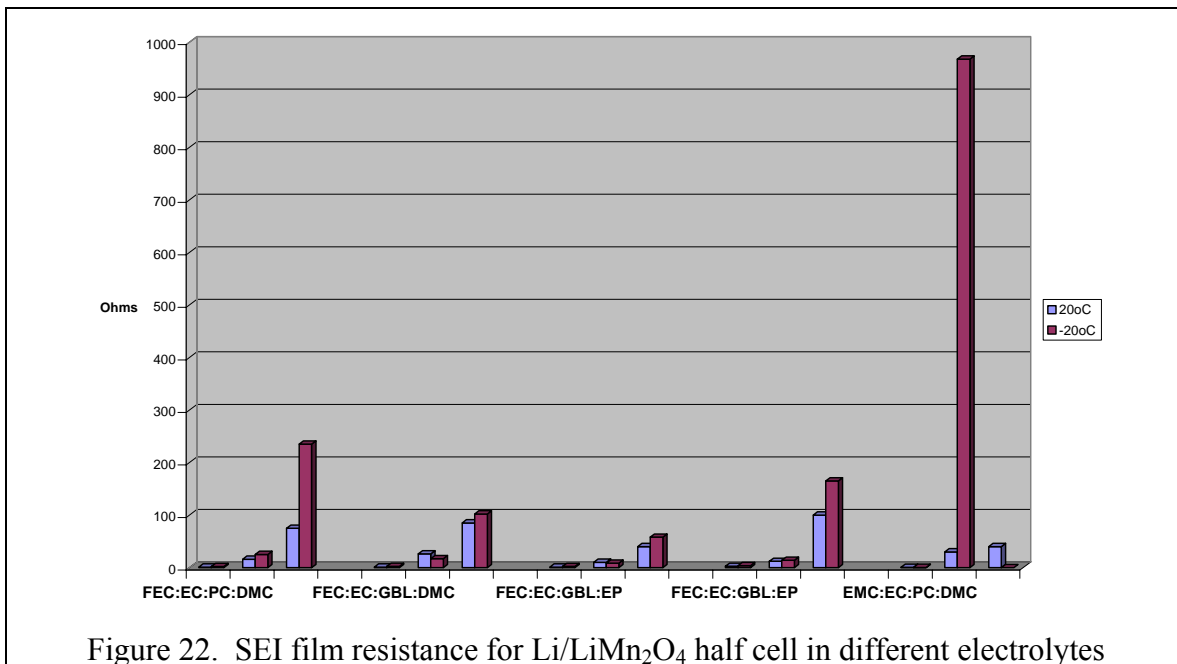
Figure 22. SEI film resistance for Li/LiMn$_2$O$_4$ half cell in different electrolytes

The SEI impedance spectra and the simulation results for LiMn$_2$O$_4$ anode are reported in Figures 23 to 27. In FEC electrolytes, there is not much change in SEI film impedance when the cell operated at the low temperature of –20°C. Conversely, for the baseline

electrolyte, there is a significant increase in interfacial impedance when the cell operates at -20°C.

Figure 23. Li/ LiMn$_2$O$_4$ w/ 10% C in 1.2M LiPF$_6$ FEC:EC:PC:DMC (10:20:10:60)

Charge; Impedance at RT	Charge; Impedance at -20°C
Ohmic Resistance: 1.1 Charge Transfer Resistance: 16 Interface Film Resistance: 75	Ohmic Resistance: 2 Charge Transfer Resistance: 25 Interface Film Resistance: 235
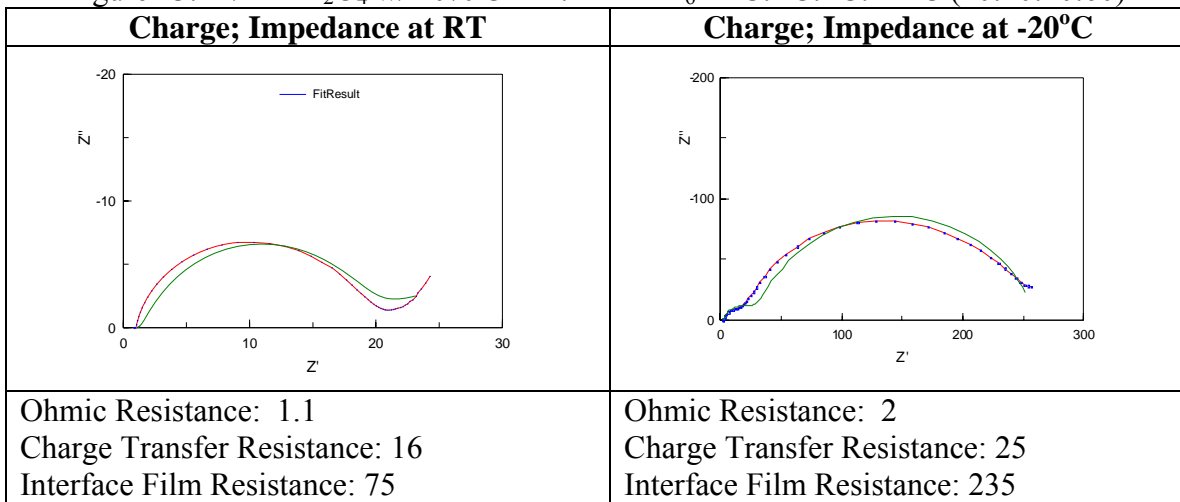
Figure 24. Li/ LiMn$_2$O$_4$ w/ 10% C in 1.2M LiPF$_6$ FEC:EC:GBL:DMC (10:15:20:55)

Charge; Impedance at RT	Charge; Impedance at -20°C
Ohmic Resistance: 0.9 Charge Transfer Resistance: 26 Interface Film Resistance: 85	Ohmic Resistance: 2.3 Charge Transfer Resistance: 17 Interface Film Resistance: 102
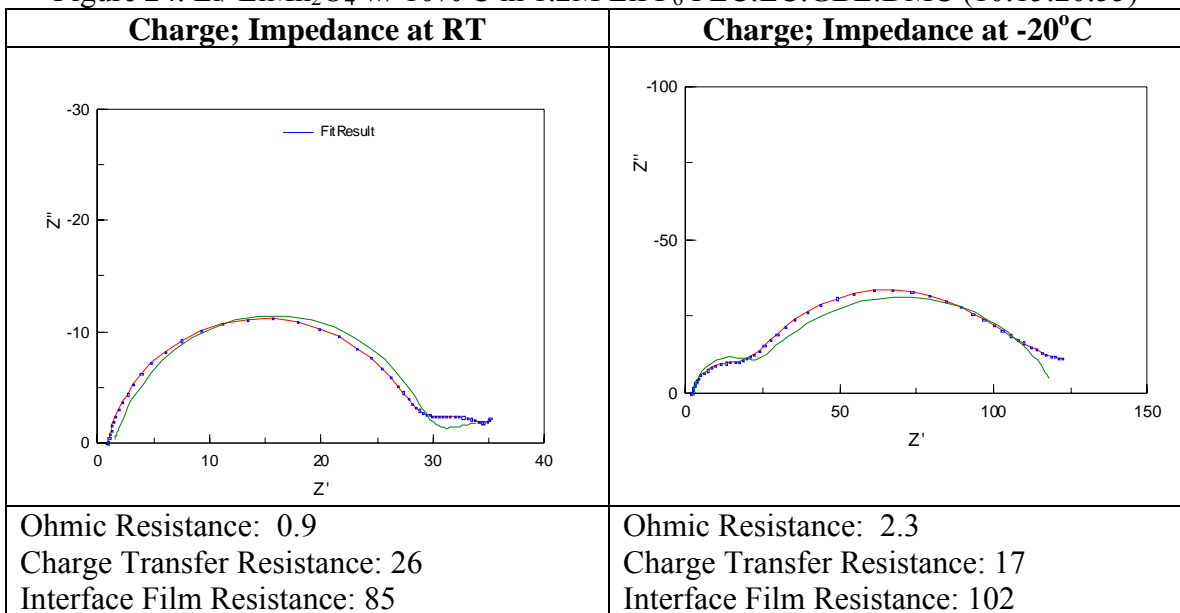
Figure 25. Li/ LiMn$_2$O$_4$ w/ 10% C in 1.2M LiPF$_6$ FEC:EC:GBL:EP (10:15:25:50)

Charge; Impedance at RT	Charge; Impedance at -20°C
Ohmic Resistance: 1.1 Charge Transfer Resistance: 10 Interface Film Resistance: 40	Ohmic Resistance: 2.2 Charge Transfer Resistance: 8.5 Interface Film Resistance: 58
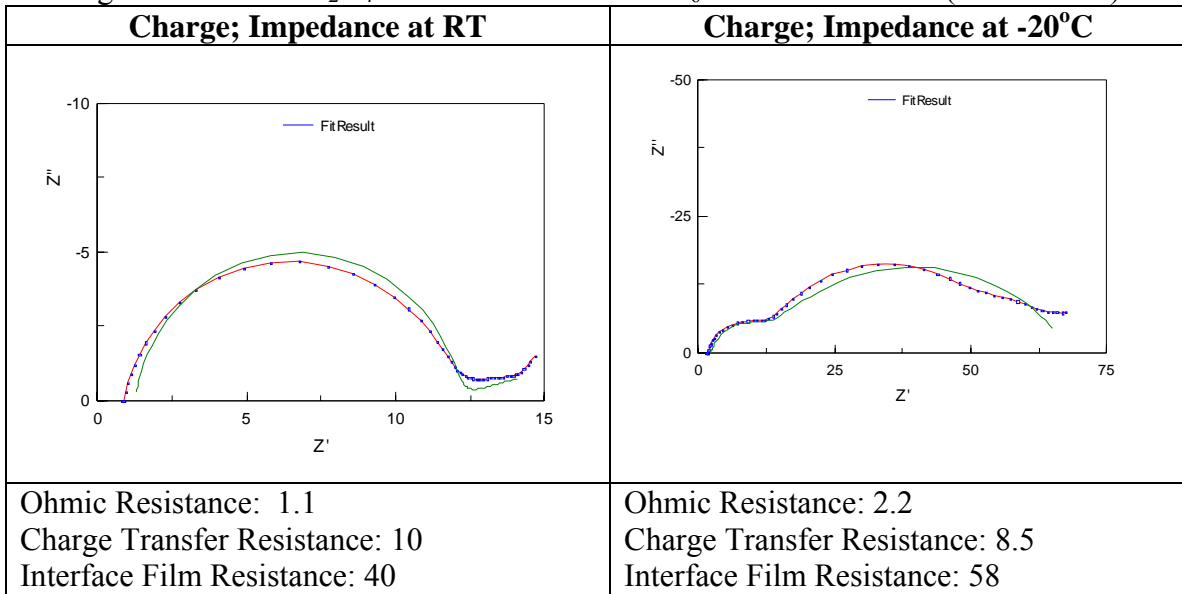
Figure 26. Li/ LiMn$_2$O$_4$ w/ 10% C in 0.8M + 0.4M LiBF$_4$ in LiPF$_6$ FEC:EC:GBL:EP (10:15:25:50)

Charge; Impedance at RT	Charge; Impedance at -20°C
Ohmic Resistance: 2.6 Charge Transfer Resistance: 12 Interface Film Resistance: 100	Ohmic Resistance: 3.8 Charge Transfer Resistance: 14 Interface Film Resistance: 165
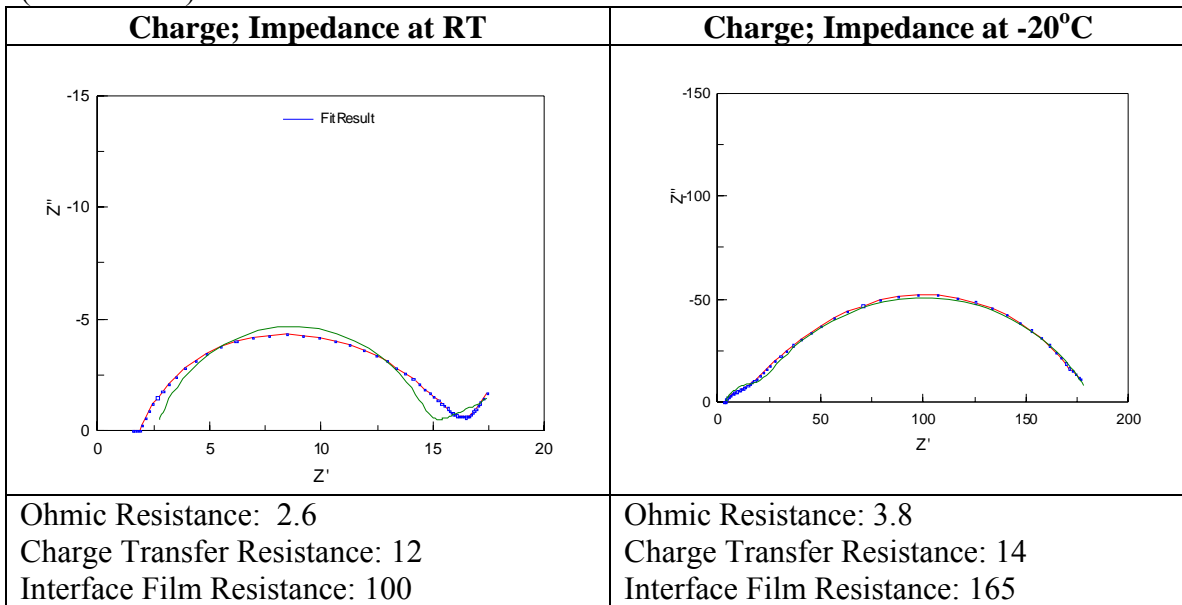
Figure 27. Li/ LiMn$_2$O$_4$ w/ 10% C in 1.2M LiPF$_6$ in EMC:EC:PC:DMC (10:20:10:60)

Charge; Impedance at RT	Charge; Impedance at -20$^{\text{o}}$C
Ohmic Resistance: 0.5 Charge Transfer Resistance: 30 Interface Film Resistance: 40	Ohmic Resistance: 0.4 Charge Transfer Resistance: 968 Interface Film Resistance: 0
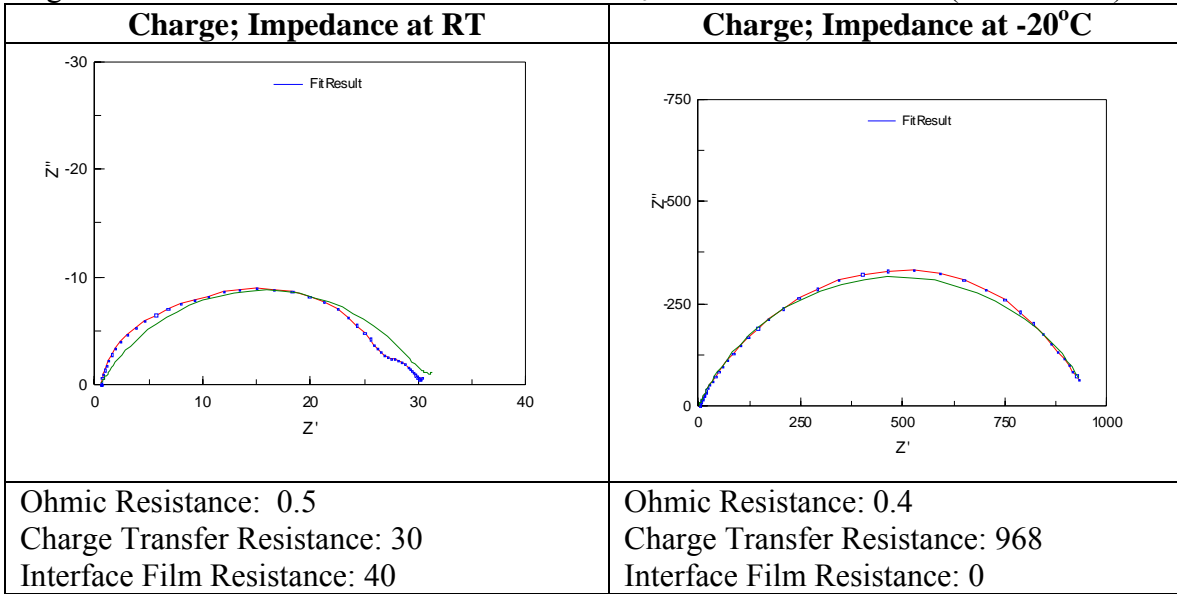
3.2.5 <u>AC Impedance Analysis of LiMn$_{1/3}$Ni$_{1/3}$Co$_{1/3}$O$_2$ (NMC) Cathode Material</u>

The SEI film resistance for Al-doped LiMn$_2$O$_4$ cathode in half-cell configuration is reported in Figure 28. AC impedance measurements were taken with the cells in fully charge state.
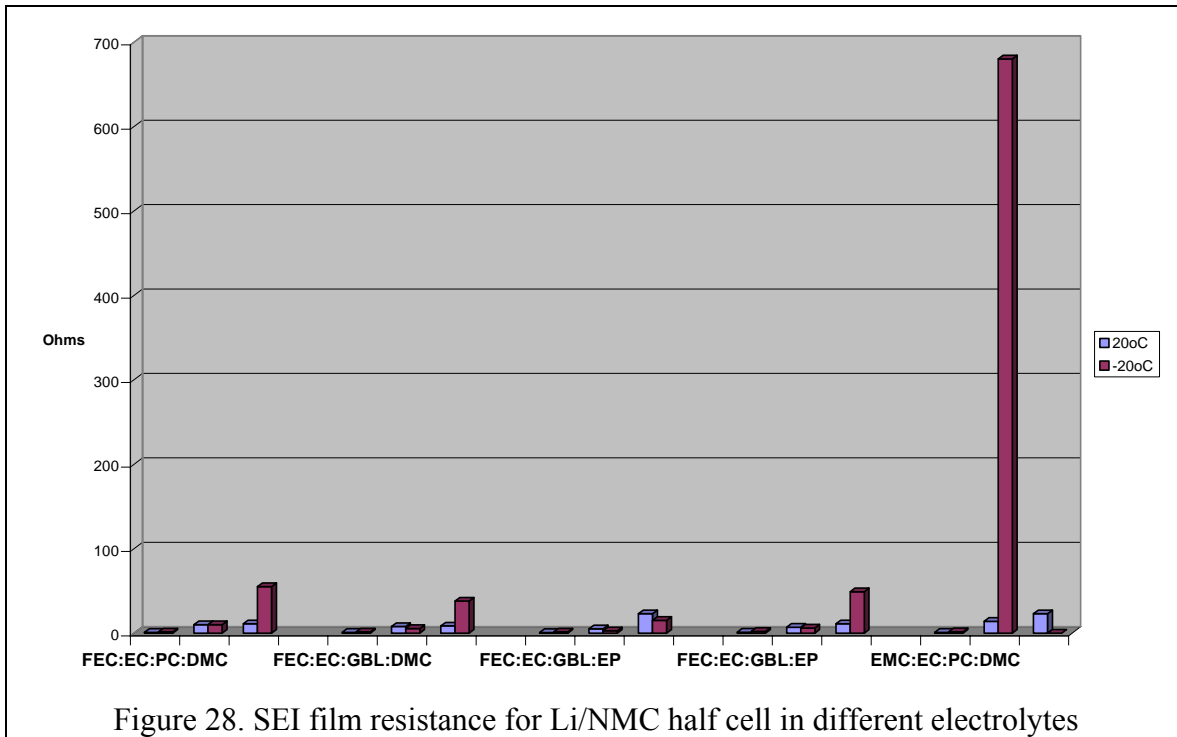

Figure 28. SEI film resistance for Li/NMC half cell in different electrolytes

For NMC cathode materials, the SEI impedance values at –20$^{\text{o}}$C in FEC electrolytes are very small, compare to the baseline electrolyte. This clearly suggested that FEC also has

a strong effect in the formation of SEI film on the cathode material. The SEI impedance spectra and the simulation results for $LiMn_2O_4$ anode are reported in Figures 29 to 33.

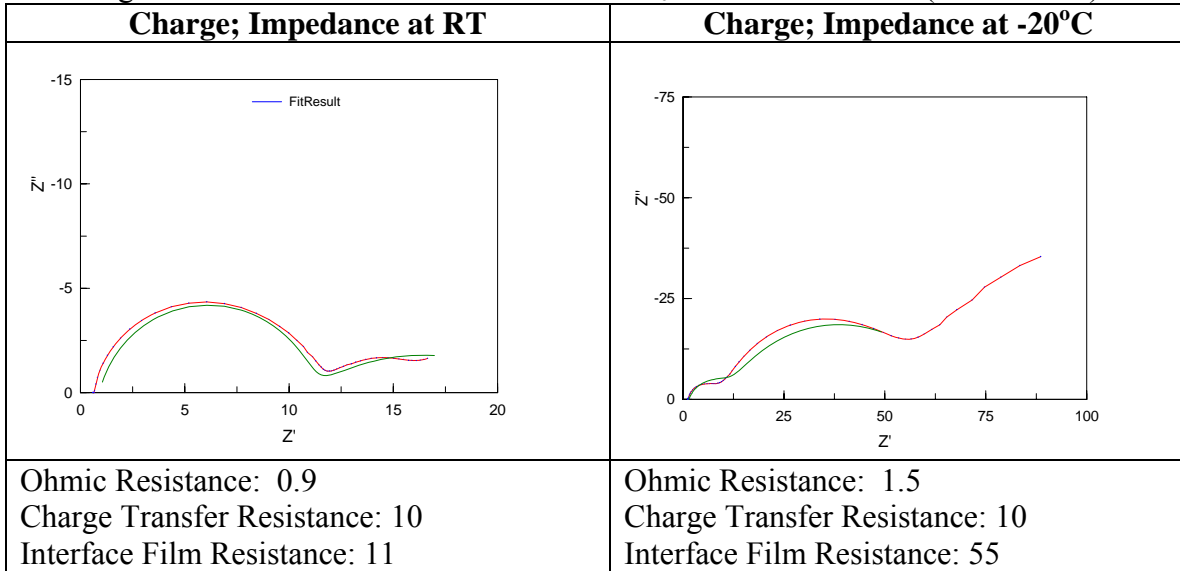Figure 29. Li/NCM w/ 10% C in 1.2M $LiPF_6$ FEC:EC:PC:DMC (10:20:10:60)

Charge; Impedance at RT	Charge; Impedance at -20°C
Ohmic Resistance: 0.9 Charge Transfer Resistance: 10 Interface Film Resistance: 11	Ohmic Resistance: 1.5 Charge Transfer Resistance: 10 Interface Film Resistance: 55

Figure 30. Li/NCM w/ 10% C in 1.2M $LiPF_6$ FEC:EC:GBL:DMC (10:15:20:55)

Charge; Impedance at RT	Charge;Impedance at -20°C
Ohmic Resistance: 0.8 Charge Transfer Resistance: 7.8 Interface Film Resistance: 8.5	Ohmic Resistance: 1.5 Charge Transfer Resistance: 5.5 Interface Film Resistance: 38
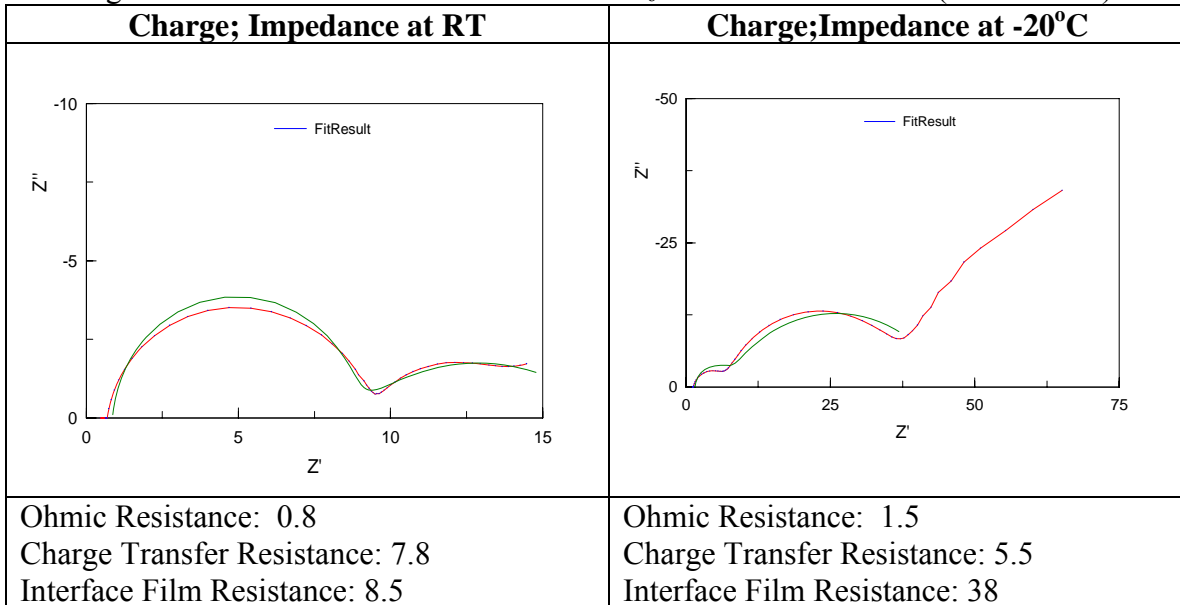
Figure 31. Li/NCM w/ 10% C in 1.2M LiPF6 FEC:EC:GBL:EP (10:15:25:50)

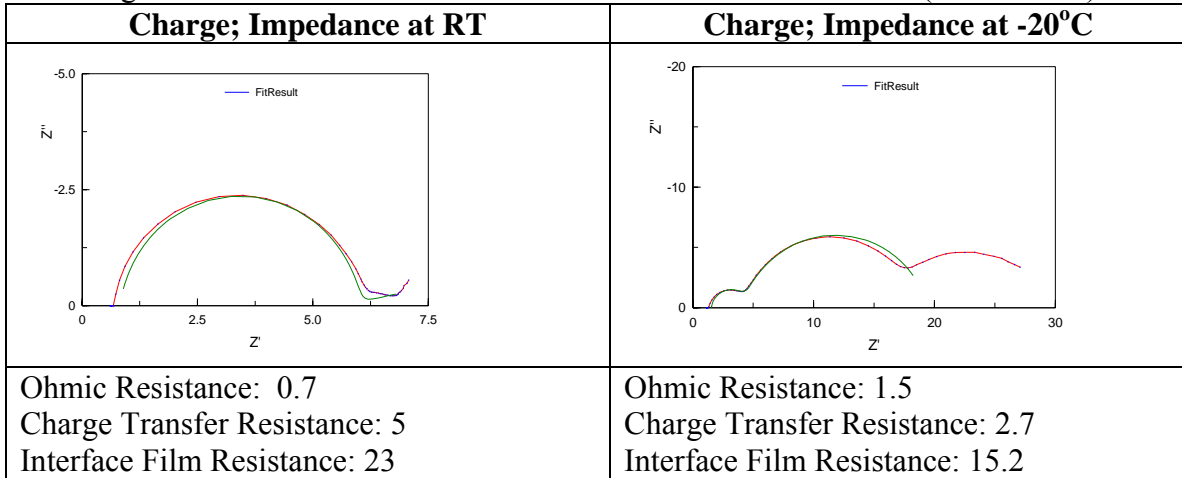| Charge; Impedance at RT	Charge; Impedance at -20°C
Ohmic Resistance: 0.7 Charge Transfer Resistance: 5 Interface Film Resistance: 23	Ohmic Resistance: 1.5 Charge Transfer Resistance: 2.7 Interface Film Resistance: 15.2

Figure 32. Li/NCM w/ 10% C in 0.8M + 0.4M LiBF$_4$ in LiPF$_6$ FEC:EC:GBL:EP (10:15:25:50)

Charge; Impedance at RT	Charge; Impedance at -20°C
Ohmic Resistance: 1.1 Charge Transfer Resistance: 7 Interface Film Resistance: 11	Ohmic Resistance: 2.2 Charge Transfer Resistance: 6 Interface Film Resistance: 49
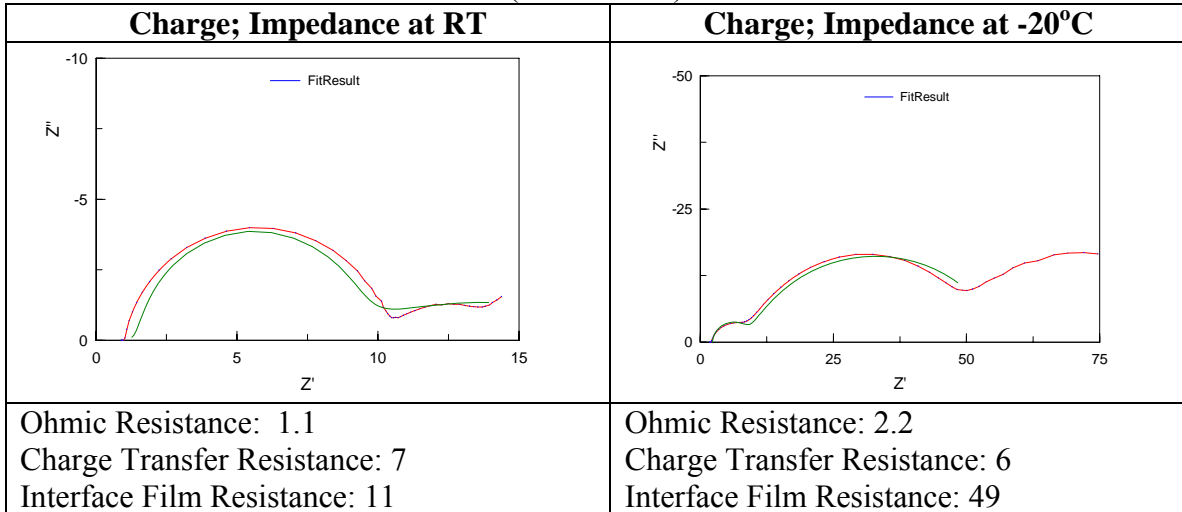
Figure 33. Li/NCM w/ 10% C in 1.2M LiPF$_6$ in EMC:EC:PC:DMC (10:20:10:60)

Charge; Impedance at RT	Charge; Impedance at -20°C
Ohmic Resistance: 0.9 Charge Transfer Resistance: 14 Interface Film Resistance: 23	Ohmic Resistance: 1.6 Charge Transfer Resistance: 680 Interface Film Resistance: 0
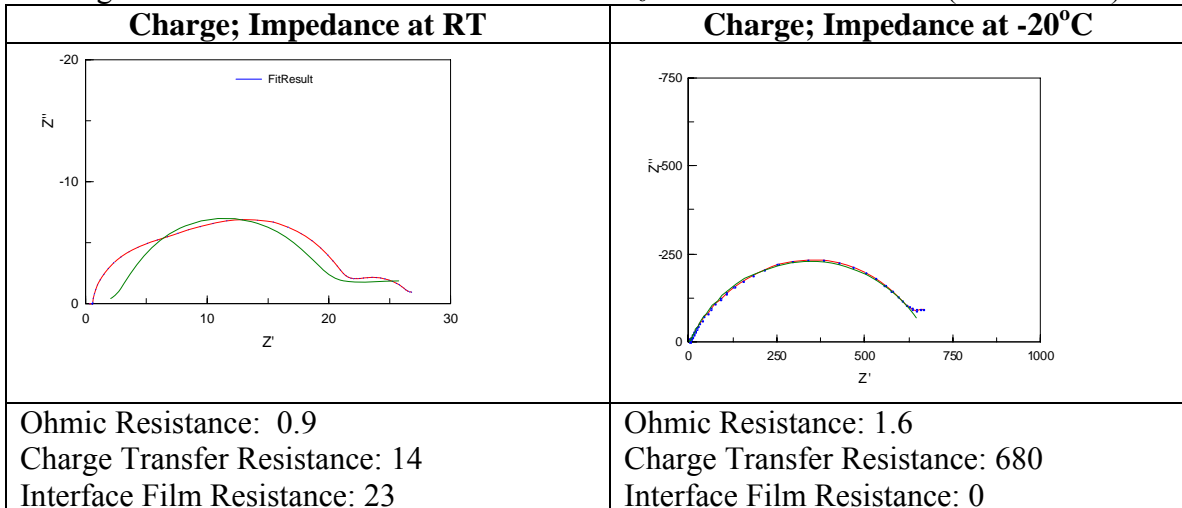
3.2.5 AC Impedance Analysis of Full Cells

Full cells with MCMB/G1520P anodes and NMC/Al-doped $LiMn_2O_4$ have been fabricated to measure the SEI film resistance. The full cells are filled with FEC:EC:GBL:EP (10:15:25:50) electrolyte which has shown to have excellent film forming properties. AC impedance measurements were taken with the cells in fully charge state.

Figure 34. SEI film resistance for full cell in FEC:EC:GBL:EP electrolytes
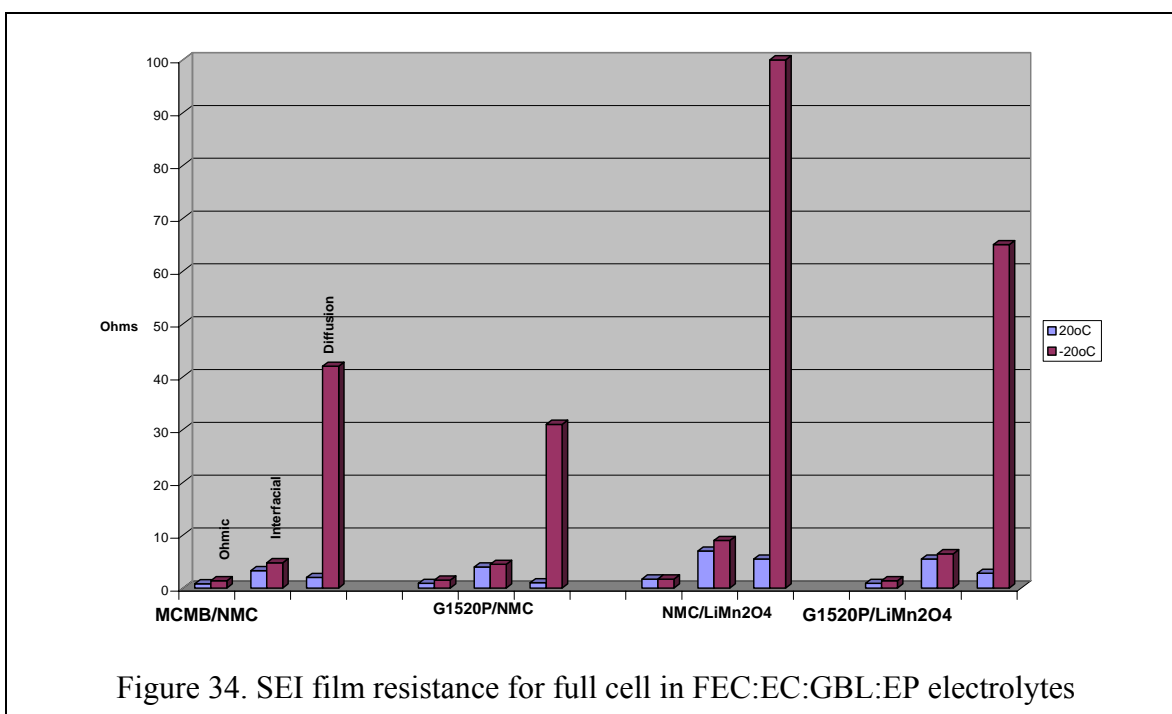
The results for the full cells impedance analysis reported in Figure 34 indicated that the interfacial film resistance values of the full cells are fairly much insensitive to temperature change. The diffusion resistance did increase at the low temperature of −20°C and MCMB cells showed higher resistance value than surface treated graphite G1520P.

The SEI impedance spectra and the simulation results for $LiMn_2O_4$ anode are reported in Figures 35 to 38.

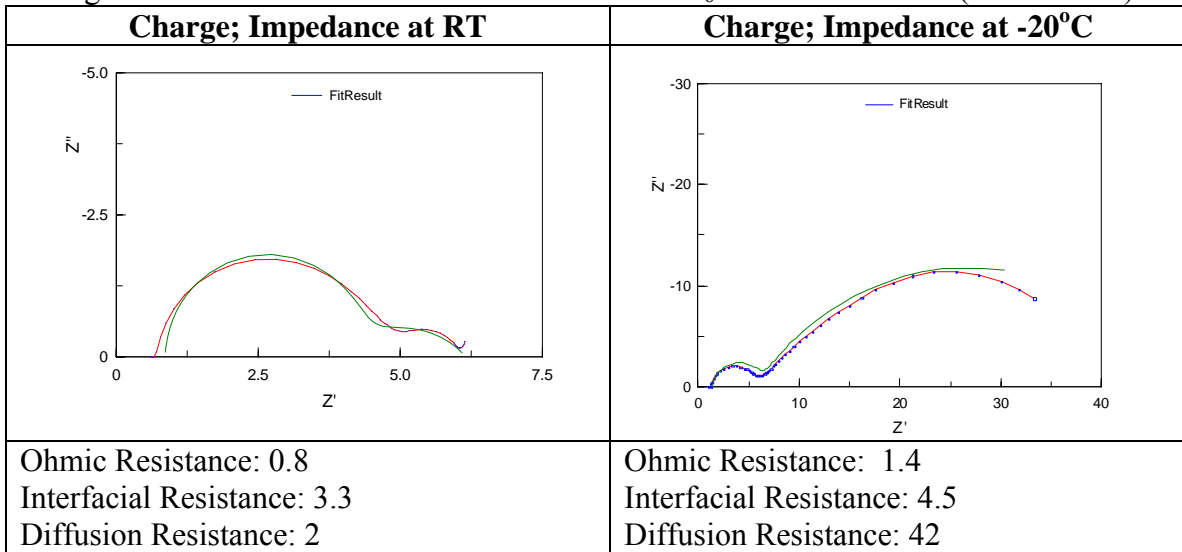Figure 35. MCMB/ NMC w/ 10% C in 1.2M LiPF$_6$ FEC:EC:GBL:EP (10:15:25:50)

Charge; Impedance at RT	Charge; Impedance at -20°C
Ohmic Resistance: 0.8 Interfacial Resistance: 3.3 Diffusion Resistance: 2	Ohmic Resistance: 1.4 Interfacial Resistance: 4.5 Diffusion Resistance: 42

Figure 36. G1520P/ NMC w/ 10% C in 1.2M LiPF$_6$ FEC:EC:GBL:EP (10:15:25:50)

Charge; Impedance at RT	Charge; Impedance at -20°C
Ohmic Resistance: 0.9 Interfacial Resistance: 4 Diffusion Resistance: 1	Ohmic Resistance: 1.5 Interfacial Resistance: 4.5 Diffusion Resistance: 31
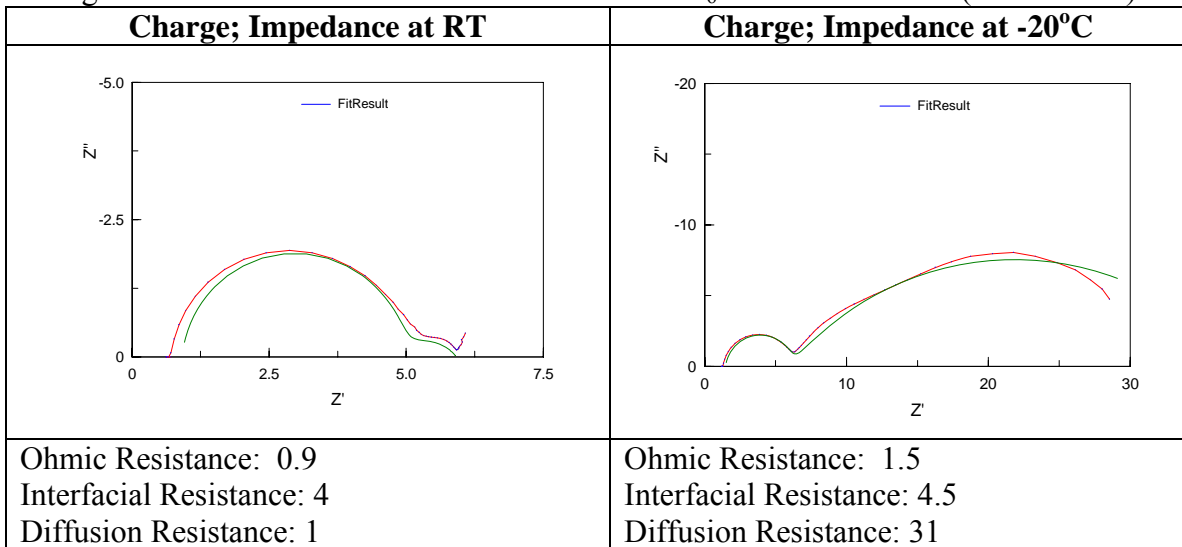
Figure 37. MCMB/ LiMn$_2$O$_4$ w/ 10% C in 1.2M LiPF$_6$ FEC:EC:GBL:EP (10:15:25:50)

Charge; Impedance at RT	Charge; Impedance at -20°C
Ohmic Resistance: 1.7 Interfacial Resistance: 7 Diffusion Resistance: 5.5	Ohmic Resistance: 1.7 Interfacial Resistance: 9 Diffusion Resistance: 100
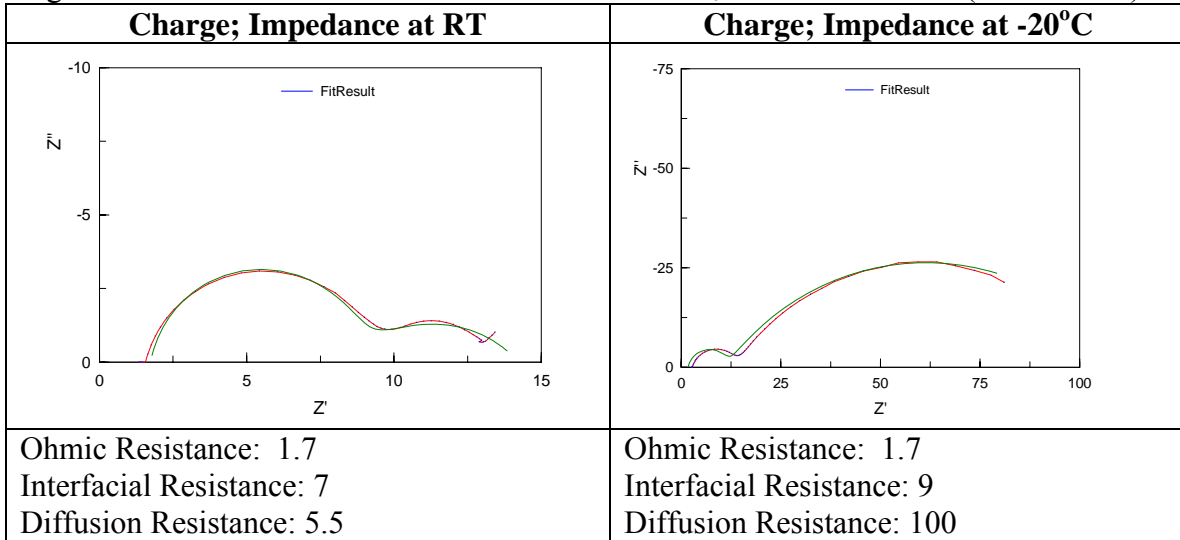
Figure 38. G1520P/ LiMn$_2$O$_4$ w/ 10% C in 1.2M LiPF$_6$ FEC:EC:GBL:EP (10:15:25:50);

harge; Impedance at RT	Charge; Impedance at -20°C
Ohmic Resistance: 0.9 Interfacial Resistance: 5.5 Diffusion Resistance: 2.8	Ohmic Resistance: 1.4 Interfacial Resistance: 6.5 Diffusion Resistance: 65
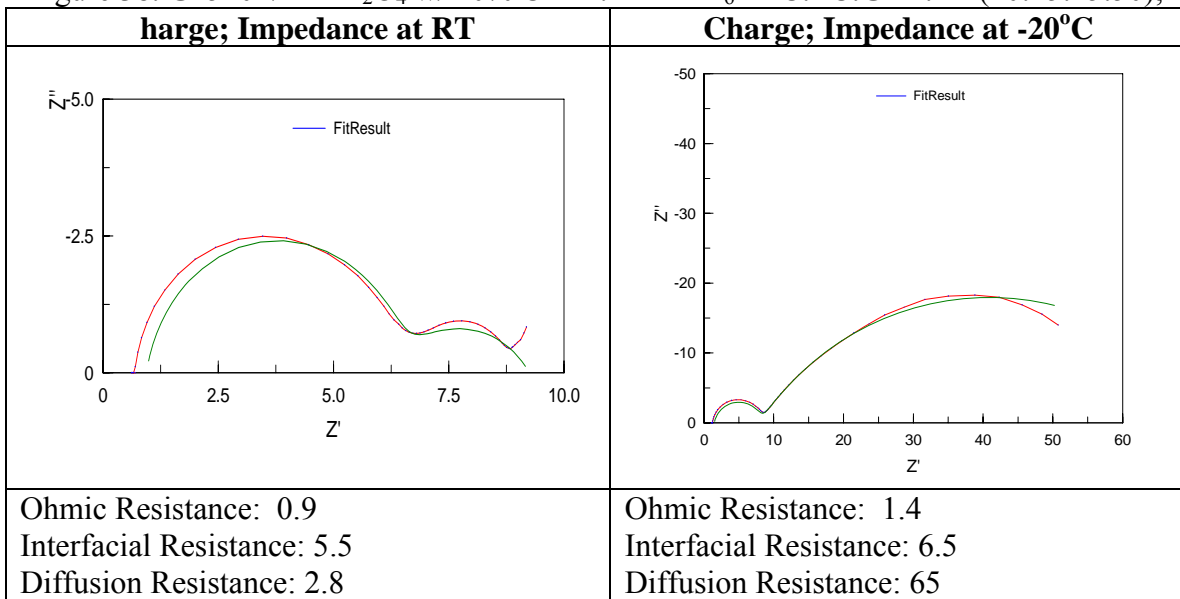
4- Conclusion

The results of our Phase I work indicated that the interfacial impedance of Fluoro Ethylene Carbonate (FEC) containing electrolytes at the low temperature of –20°C is astonishingly low compared to the baseline 1.2M LiPF$_6$ EMC:EC:PC:DMC (10:20:10:60) electrolyte. We found that electrolyte formulations with fluorinated-carbonate co-solvent have excellent film forming properties and better de-solvation characteristics to decrease the interfacial SEI film resistance and facilitate the Li-ion diffusion across the SEI film. For example, the interfacial resistances for Li/MCMB half cell in 1.2M LiPF$_6$ FEC:EC:GBL:EP (10:15:25:50) are respectively 0.9Ω at both 20°C and -20°C. For the baseline electrolyte EC:EMC:PC:DMC, the interfacial resistances are respectively 23Ω and 950 Ω at 20°C and -20°C. The very overwhelming low interfacial

impedance for FEC electrolyte will translate into higher power for cold cranking and higher Regen charge for Li-ion cell at low temperature. Our result is supported by theory using the Advanced Electrolyte Model developed by our collaborators at DOE Idaho National Laboratories (INL).

The benefits of the formation of low interfacial impedance SEI film in FEC based electrolytes are three fold:
1. Improve the cold-cranking performance of Li-ion cell at the low temperature range
2. Increase the Li intercalation kinetic through the low interfacial impedance film during Regen/charge thus preventing Li plating problem on the anode at low temperature
3. FEC electrolyte has lower flammability and hence safer

The successful outcome of this program will be the development of new electrolyte that can form low impedance SEI film on high power Li-ion battery at the low temperature of $-20^{\circ}C$. Low cell impedance will translate into Li-ion cell capable of meeting DOE requirement for cold cranking at the low temperature. Reaching this milestone is very critical for the implementation of Li-ion battery in the HEV commercial market. Further, since fluorinated electrolyte has low flammability, the resulting Li-ion cell can be made safer.

References

[1] H. Lin, D. Chua, M. Salomon, H.C. Shiao, M. Hendrickson, E. Plichta, and S. Slane, Electrochem. Solid-State Lett., 4, A71 (2001)

[2] Private communication by Lars Valoen at E1 Moli

[3] H.-G. Schweiger et al., *J. Electrochem. Soc.*, 152 (3), A577-A582 (2005))

[4] S. V. Sazhin, M. Y. Khimchenko, Y. N. Tritenichenko, and H. S. Lim, *J. Power Sources*, **87,** 112 (2000)

[5] M. C. Smart, B. V. Ratnakumar, and S. Surampudi, *J. Electrochem. Soc.*, **149** (4), A361 (2002)

[6] A. Ohta, H. Koshina, H. Okuno, and H. Murai, *J. Power Sources*, **54,** 6 (1995))

[7] M. Kobayashi, et al.*, J. Fluorine Chemistry,* Vol. 120 (2), 105-110 (2003))

[8] M.C. Smart, B.V. Ratnakumar, S. Surampudi, Y. Wang, X. Zhang, S.G. Greenbaum, A. Hightower, C.C. Ahn, and B. Fultz, J. Electrochem. Soc., 146, 3963 (1999)

[9] Z. Wang, X. Huang and L. Chen, J. Elecrochem. Soc., 151, A1641 (2004)